U.S. Department of Energy
Energy Efficiency and Renewable Energy
Bringing you a prosperous future where energy is clean, abundant, reliable, and affordable

Industrial Technologies Program

Industrial Materials for the Future

Final Technical Report

Development of Cost-Effective Low-Permeability Ceramic and Refractory Components for Aluminum Melting and Casting

December 2005

Principal Investigators:

Dale E. Brown
Pyrotek, Inc.

Ronald D. Ott
Oak Ridge National Laboratory

Jeffrey D. Smith
University of Missouri—Rolla

Managed by
UT-Battelle, LLC

ORNL/TM-2005/266

FINAL TECHNICAL REPORT

Project Title:	Development of Cost-Effective Low-Permeability Ceramic and Refractory Components for Aluminum Melting and Casting
Award No:	DE-FC36-01ID14244
Project Period:	August 1, 2002–July 31, 2005
PIs:	Dale E. Brown (Pyrotek, Inc., Jackson, TN) Now at Pyrotek, Elmsford, NY (914) 345-4745 dalbro@pyrotek-snif.com Ronald D. Ott (Oak Ridge National Laboratory) (865) 574-5172 ottr@ornl.gov Jeffrey D. Smith (University of Missouri—Rolla) (573) 341-4447 jsmith@umr.edu
Additional Researchers:	Greg Hodren (Pyrotek, Inc.) (717) 249-2075 grehod@pyrotek-inc.com Puja B. Kadolkar **(**Oak Ridge National Laboratory) (865) 574-9956 kadolkarpb@ornl.gov William G. Fahrenholtz (University of Missouri—Rolla) (573) 341-6343 billf@umr.edu
Recipient Organization:	Pyrotek, Inc. 1231 Manufacturers Row Trenton, TN 38382
National Laboratory:	Oak Ridge National Laboratory Bethel Valley Road P.O. Box 2008 Oak Ridge, TN 37831
Subcontractor:	University of Missouri at Rolla Department of Materials Science and Engineering 223 McNutt Hall Rolla, MO 65409

ORNL/TM-2005/266

Development of Cost-Effective Low-Permeability Ceramic and Refractory Components for Aluminum Melting and Casting

Dale E. Brown
Greg Hodren
Pyrotek, Inc.

Ronald D. Ott
Puja B. Kadolkar
Oak Ridge National Laboratory

Jeffrey D. Smith
William G. Fahrenholtz
University of Missouri—Rolla

December 2005

Prepared by
OAK RIDGE NATIONAL LABORATORY
P.O. Box 2008
Oak Ridge, Tennessee 37831-6283
managed by
UT-Battelle, LLC
for the
U.S. DEPARTMENT OF ENERGY
under contract DE-AC05-00OR22725

Acknowledgments and Disclaimer

Acknowledgments

This report is based upon work supported by the U.S. Department of Energy, Energy Efficiency and Renewable Energy, Industrial Technologies Program, Industrial Materials for the Future, under Award No. DE-FC36-01ID14244.

The authors would like to acknowledge Terry Tiegs, Jim Kiggans, Vinod Sikka, Jackie Mayotte, and David Harper at ORNL for their valuable contributions to and participation in the project. In addition, support from Soto Jose Maria and Sander Todd Pearson of the University of Missouri—Rolla is greatly appreciated. The authors would like to thank Dr. Peter Angelini for project guidance and review.

Oak Ridge National Laboratory is operated by UT-Battelle, LLC, for the U.S. Department of Energy under contract DE-AC05-00OR22725.

Contents

List of Figures

List of Tables

Abbreviations and Acronyms

Al_2O_3	alumina
BN	boron nitride
Btu	British thermal unit
CTE	coefficient of thermal expansion
DFS	dense fused silica
DOE	U.S. Department of Energy
EDS	energy-dispersive spectroscopy
EDX	energy-dispersive X-ray
IMF	Industrial Materials for the Future (DOE)
IR	infrared
LPD	low-pressure die
MECS	Manufacturing Energy Consumption Survey
NO_x	nitrogen dioxide
OIT	Office of Industrial Technologies (DOE)
ORNL	Oak Ridge National Laboratory
OTT	Office of Transportation Technologies (DOE)
PSD	particle size distribution
SEM	scanning electron microscope
SiO_2	silica
UMR	University of Missouri—Rolla
YAG	yttrium aluminum garnet

1. Executive Summary

1.1 Research and Development

A recent review by the U.S. Advanced Ceramics Association, the Aluminum Association, and the U.S. Department of Energy's Office of Industrial Technologies (DOE/OIT) described the status of advanced ceramics for aluminum processing, including monolithics, composites, and coatings. The report observed that monolithic ceramics (particularly oxides) have attractive properties such as resistance to heat, corrosion, thermal shock, abrasion, and erosion [1]. However, even after the developments of the past 25 years, there are two key barriers to commercialization: reliability and cost-effectiveness. Industry research is therefore focused on eliminating these barriers. Ceramic coatings have likewise undergone significant development and a variety of processes have been demonstrated for applying coatings to substrates. Some processes, such as thermal barrier coatings for gas turbine engines, exhibit sufficient reliability and service life for routine commercial use.

Worldwide, aluminum melting and molten metal handling consumes about 506,000 tons of refractory materials annually. Refractory compositions for handling molten aluminum are generally based on dense fused cast silica or mullite. The microstructural texture is extremely important because an interlocking mass of coarser grains must be bonded together by smaller grains in order to achieve adequate strength. At the same time, well-distributed microscopic pores and cracks are needed to deflect cracks and prevent spalling and thermal shock damage [2].

The focus of this project was to develop and validate new classes of cost-effective, low-permeability ceramic and refractory components for handling molten aluminum in both smelting and casting environments. The primary goal was to develop improved coatings and functionally graded materials that will possess superior combinations of properties, including resistance to thermal shock, erosion, corrosion, and wetting. When these materials are successfully deployed in aluminum smelting and casting operations, their superior performance and durability will give end users marked improvements in uptime, defect reduction, scrap/rework costs, and overall energy savings resulting from higher productivity and yield. The implementation of results of this program will result in energy savings of 30 trillion Btu/year by 2020.

For this Industrial Materials for the Future (IMF) project, riser tube used in the low-pressure die (LPD) casting of aluminum was selected as the refractory component for improvement. In this LPD process, a pressurized system is used to transport aluminum metal through refractory tubes (riser tubes) into wheel molds. It is important for the tubes to remain airtight because otherwise, the pressurized system will fail. Generally, defects such as porosity in the tube or cracks generated by reaction of the tube material with molten aluminum lead to tube failure, making the tube incapable of maintaining the pressure difference required for normal casting operation. Therefore, the primary objective of the project was to develop a riser tube that is not only resistant to thermal shock, erosion, corrosion, and wetting, but is also less permeable, so as to achieve longer service life. Currently, the dense-fused silica (DFS) riser tube supplied by Pyrotek lasts for only 7 days before undergoing failure.

The following approach was employed to achieve the goal:

- Develop materials and methods for sealing surface porosity in thermal-shock-resistant ceramic refractories

- Develop new ceramic coatings for extreme service in molten aluminum operations, with particular emphasis on coatings based on highly stable oxide phases
- Develop new monolithic refractories designed for lower-permeability applications using controlled porosity gradients and particle size distributions
- Optimize refractory formulations to minimize wetting by molten aluminum, and characterize erosion, corrosion, and spallation rates under realistic service conditions
- Scale up the processing methods to full-sized components and perform field testing in commercial aluminum casting shops

1.2 Accomplishments

Two cost-effective coating formulations that offered excellent thermal shock properties and resistance to molten aluminum attack were identified as promising candidates for application on DFS riser tubes. One coating formulation, called "XL" glaze, is a zircon-based coating material system developed at Pyrotek, Inc. The other glaze, referred to as "glaze 1," is a lithium-silicate-based coating system that was investigated at Oak Ridge National Laboratory (ORNL). In addition to coating formulations, a computer model suggesting optimized particle packing or particle size distribution (PSD) that would minimize permeability in monolithic fused silica castables was developed at the University of Missouri—Rolla (UMR). Another outcome that evolved out of the research efforts at UMR was development of a permeability measuring apparatus that can accommodate a full-scale DFS riser tube. Currently, DFS riser tubes coated with Pyrotek's XL glaze are routinely manufactured and supplied by Pyrotek to its customers. The XL-coated DFS tubes are reported to last 3 to 5 weeks, as compared to uncoated DFS tubes, which last only 7 days, indicating that the XL coating extends the life of the DFS tubes up to 300–400%. Additionally, four full-scale fused silica castables that were formulated on the basis of the PSD computer model were designed and manufactured at Pyrotek and are now undergoing field testing at General Aluminum, Wapakoneta, Ohio. Preliminary test results have shown that the silica castables lasted for 8 weeks during the aluminum casting operations, indicating an increase in the life of the riser tubes of 700%. The potential national energy savings by replacing the older riser tube with this improved riser tube is estimated to be 206 billion Btu/year.

1.3 Commercialization

Pyrotek, Inc., is currently leading the commercialization efforts in promoting the new riser-tube castables as well as the new glaze systems through its own clientele. Pyrotek is one of the world's leading suppliers of consumable products and melt treatment solutions for the aluminum industry and has about 60 manufacturing sites, sales offices, and warehouses worldwide. Pyrotek has already sold about 1200 of their XL-coated DFS riser tubes and has reported an increasing number of inquiries since 2003 that suggests growing awareness of these enhanced riser tubes within the refractory and aluminum industrial community. Pyrotek is projecting better sale numbers with the production of their fused silica castables, which have been shown to increase the life of riser tubes by 700%.

1.4 Recommendations

It is recommended that use of coatings and castable formulations similar to those studied in this project be extended to other refractory components within the aluminum casting industry (such as troughs, metal handling ladles, spouts and pins), as well within other industries, including glass, chemical, petrochemical, steel, agriculture, mining, and forest products.

2. Introduction

2.1 Current Status of Refractories in Industrial Processing

Refractories are used in many industries, including glass, aluminum, chemical, metalcasting, petrochemicals, steel, agriculture, mining, and forest products. Refractory materials are used primarily in applications requiring corrosion resistance at high temperatures. Thus, they are generally used as insulation or containment linings for various furnaces, boilers, and reactor vessels used in different industries. The purpose of refractories is generally to contain heat, melts, or chemicals, and therefore they play a vital role in all energy-intensive industries. A recent study performed by DOE/OIT; ORNL; Metals Manufacture, Process, and Controls Technology, Inc.; and R. E. Moore and Associates, presented a detailed discussion of the refractory issues and challenges for various energy-intensive processing industries [3]. Several opportunities for energy savings through refractory improvements have been identified, and various cross-cutting R&D pathways for achieving high energy efficiency have been suggested. The research conducted through this project is a perfect example of identifying and overcoming one such cross-cutting refractory problem with a potential to provide substantial energy savings to both the aluminum and the metal casting industry.

2.2 Benefits to the Domestic Aluminum and Metal Casting Industry

The aluminum and metal casting industries are energy-intensive industries. According to the 1998 DOE Manufacturing Energy Consumption Survey (MECS) [4], 90% of the total energy consumed by these two industries is affected by refractories. Thus, it is extremely important to identify areas of refractory improvements if significant energy savings are to be realized. It has been estimated that improvement of refractory systems for the aluminum and metal casting industries could lead to energy saving opportunities up to 29.2 trillion and 8.5 trillion Btu/ year, respectively [3]. The current report discusses the energy savings that could be achieved by improving the performance of the DFS riser tubes used in the LPD casting process for the production of aluminum components. Some of the problems associated with current riser tubes are their inability to hold pressure due to high porosity and material degradation due to chemical attack from molten aluminum. Improving the performance of riser tubes will help reduce the quantity of scrap produced in the casting operation and, thus, save the energy associated with remelting of the metal scrap. Section 2.4 provides an example of how improvement in riser tubes can help the aluminum industry save 206 billion Btu of energy annually.

A multipartner research team consisting of representatives from industry (Pyrotek and its customers), a national laboratory (ORNL), and a university (UMR) conducted a systematic study to address the issues related to riser tubes and develop improved materials that would enhance the casting operation and increase production yield. Pyrotek participated by supplying the raw materials, in-process components, and finished components for experimental modification at ORNL. Pyrotek also conducted field testing, validation, scale-up, and economic analysis of the improved products. ORNL and UMR modified the refractory materials and developed new materials and processes, characterized these materials, and performed post mortem analyses in collaboration with industry. Pyrotek and its customers provided overall guidance and direction for the project by establishing R&D priorities and by monitoring research progress and deliverables. The project was very successful. Two new refractory tube formulations were developed, and one of these has been commercialized by Pyrotek.

2.3 Project Objectives

The cost-effective ceramic and refractory components for handling molten aluminum developed in this project are expected to reduce downtime through longer life, reduce scrap through lower rates of erosion and particulate generation, and reduce overall energy use by improving casting operations. These components were developed through a focused program designed to identify, develop, and understand new refractory materials; quantify their performance in molten metal service; and validate these findings through actual field testing and postmortem analysis.

The following efforts were part of this project:

- Development of autogenous materials and methods for sealing surface porosity in thermal shock–resistant fused silica refractories
- Development of new ceramic coatings for extreme service in molten aluminum operations, with particular emphasis on coatings based on YAG and other highly stable oxide phases
- Development of new monolithic refractories for creep and erosion resistance with emphasis on liquid-phase sintered mixed-oxide systems with controlled porosity gradients
- Optimization of refractory formulations to minimize wetting by molten aluminum, and characterization of erosion, corrosion, and spallation rates under realistic service conditions
- Scaleup of processing methods to full-sized components and field testing in commercial aluminum casting shops

The major issue for this project was the inability of current ceramics/refractories to maintain gas pressure in the delivery tubes for aluminum metal casting. The project focused on porosity, which can be closed either by surface modification or by changes in the bulk refractory chemistry. Both approaches were evaluated in this project. Samples of refractory materials in both finished (sintered) and green (unsintered) states were provided by Pyrotek. Both ORNL and UMR initiated efforts to formulate coatings and bulk materials. Formulation and sintering of coatings and microstructural characterization for test coupons was done at ORNL whereas formulation and sintering of coatings for full-sized components was done at Pyrotek. UMR designed new formulations, prepared fused silica castables (in the form of smaller discs) using slip casting, and conducted permeability and reactivity tests of newly formulated castables. Full-scale silica castables were manufactured at Pyrotek, while field testing and validation were performed at a commercial aluminum casting shop. Pyrotek provided advice and guidance on cost and manufacturability issues.

2.4 Assumptions and Detailed Calculations of Energy Savings (Btu) to the Domestic Aluminum Industry

Aluminum is the material of choice for many components, especially in the vehicle industry. According to *Aluminum R&D for Automotive Uses and the Department of Energy's Role*, a study performed by ORNL and DOE's Office of Transportation Technologies (OTT) in March 2000 [5], engines, transmissions, heat exchangers, and wheels account for over 83% of the aluminum currently used in vehicles in North America. Castings account for more than 75% of aluminum material used, with almost 35% of these castings produced using low-pressure methods (both low-pressure die and low-pressure permanent mold castings). Now assuming that the production demographics of 1999 represents a typical year, from a total of 3.8 billion pounds of aluminum products produced for the automotive industry each year, 1.3 billion pounds of aluminum is processed using low-pressure casting techniques. Data from Pyrotek's end users report that about 3% of the total low-pressure

castings produced are scrapped each year due to the improper performance of riser tubes during the low-pressure casting operation. The energy consumed in remelting this scrap and the energy lost in the associated dross formation account to an annual savings of 203 billion Btu. In addition, replacement of the original DFS tubes with improved, longer-lasting, castable tubes is estimated to provide additional annual energy savings of up to 2.19 billion Btu. Longer-lasting riser tubes suggest fewer replacements and fewer tubes consumed per year. With fewer tubes consumed per year, fewer tubes have to be produced. This additional 2.19 billion Btu in energy savings relates to the energy associated with the reduced DFS riser tube production. Table 2.1 shows the detailed calculation of the energy savings. It is important to note that these energy calculations do not incorporate the sources of energy losses outside the casting process, such as die preheating and heating of the holding furnace during the downtime involved with tube replacement. Adding these losses will further help enhance the energy savings in the casting operation.

Table 2.1. Energy savings in the low-pressure casting of aluminum components due to improved riser tubes

Item no.	Item	
1	Annual production of aluminum automotive components produced using low-pressure casting processes, lb [a]	1.33×10^9
2	Annual production of scrap metal (3%) due to improper functioning of the riser tube, lb	3.99×10^7
3	Annual natural gas energy consumption in remelting scrap, Btu[b]	8.78×10^{10}
4	Annual loss of metal in dross formation during remelting (4%), lb	1.6×10^6
5	Annual energy losses due to dross formation, Btu[c]	1.16×10^{11}
6	Annual consumption of riser tubes by low-pressure casters in U.S., lb	9.0×10^5
7	Annual natural gas energy consumption during firing of riser tubes, Btu[d]	2.5×10^9
8	Annual energy savings due to reduced riser tube production, Btu[e]	2.19×10^9
9	Total energy savings (adding Item 3 + Item 5 + Item 8)	2.06×10^{11}
	Total energy savings	**2.06×10^{11}**

[a] Data from Ref. [5].

[b] Typical energy consumed by a reverberatory aluminum-melting furnace with an efficiency of 23% is 2200 Btu/lb [3].

[c] According to the 1997 energy and environmental profile of the U.S. aluminum industry [6], the energy required to produce aluminum from ore is about 72500 Btu/lb.

[d] Natural gas consumption is 2778 Btu/lb of refractory material fired (Pyrotek).

[e] With Pyrotek's castable riser tubes lasting 8 weeks longer, the annual production of riser tubes decreases by a factor of 8.

3. Background

The goal of this multipartner research project was to develop and validate new classes of cost-effective refractory components for handling molten aluminum in casting environments. This was done by emphasizing candidate materials and processes based on scientifically sound applications of new ceramic compositions and novel processing capabilities. The project was built on ORNL's expertise in ceramic forming (particularly gelcasting), mixed-oxide refractories and coatings, and rapid thermal processing. It also benefited from ORNL's state-of-the-art materials characterization facilities.

Oxide refractories for handling molten aluminum are generally made from either fused silica or mullite. The components are usually not sintered to full density because experience has shown that some porosity contributes to high thermal shock resistance. For many applications, particularly in pressure casters, it is also essential that, in addition to having high thermal shock resistance, the materials not be easily wetted by the molten aluminum. The nonwetting characteristics prevent metal buildup and eventual failure in the refractory tube.

3.1 Major Project Tasks

The primary focus of this project was to develop new families of refractory ceramics, following a logical progression from low- to high-risk materials systems in the following order:

1. Autogenous coatings on fused silica, designed to seal or minimize surface porosity and gas permeability while maintaining excellent thermal shock resistance
2. Advanced ceramic coatings on fused silica, to seal surface porosity and provide exceptional resistance to erosion, corrosion, or chemical attack
3. Advanced monolithic refractories based on optimized particle packing and pore size distribution

3.1.1 Autogenous Coatings

The first major activity of the project consisted of designing cost-effective treatments to modify the surface of fused cast silica tubes. The goal was to seal surface porosity while preserving the thermal shock resistance of the bulk material. In order to make the refractory surface less permeable while keeping it resistant to molten aluminum attack, it was necessary to maintain the amorphous structure inherent in Pyrotek's fused silica refractory. This required rapid solidification of the melted surface of the refractory without allowing any crystallization to occur. ORNL's high-density plasma arc lamp was used to achieve melting and rapid solidification of fused silica. The surface-modified fused silica was examined for thickness, phase changes, and wetting by molten aluminum; the degree of porosity was estimated by measuring the gas permeability under service conditions.

3.1.2 Advanced Ceramic Coatings

The second phase of the work largely emphasized the development of mixed-oxide coatings by in situ reactions. In earlier work [7], it was found that yttrium aluminum garnet ($Y_3Al_5O_{12}$, or YAG) was exceptionally stable, as evidenced by its ability to withstand direct contact with molten lithium. YAG

is an intermediate phase (line compound) in the Y_2O_3-Al_2O_3 system [8] with eutectics on either side of the compound.

The existence of these eutectics has profound implications for the processing of this material. The line compound itself is very refractory and difficult to sinter if YAG powder is used as the starting material. But if the pure oxides are mixed and heated to a temperature above the eutectics but below the melting point of YAG, transient liquid phases form and these significantly enhance the sintering process. Once all the material has been converted to YAG, it is refractory, creep-resistant, and chemically inert.

Building on the previous results, it was proposed that YAG or YAG-like compounds formed on the surface of DFS refractories be explored. The YAG could be formed in situ by applying rare earth oxides and exploiting liquid-phase sintering to create a strong, adherent, chemically stable surface on a relatively low-cost refractory substrate. One of the biggest challenges in coating DFS refractories is their low coefficient of thermal expansion (0.5×10^{-6}/°C). One of the options considered here was to look into semicrystalline glazes with coefficients of thermal expansion (CTEs) that would match those of DFS. We selected several lithium-based silica glaze compounds with CTE values ranging from -0.9×10^{-6}/°C to 1.3×10^{-6}/°C and investigated them as possible glaze materials.

3.1.3 Advanced Monolithic Refractories

The third activity in this project consisted of developing functionally graded materials, especially density-graded, compositionally homogeneous structures [9]. Vibration-assisted slip casting was used, along with fugitive pore formers and other well-known ceramic techniques, to create refractory components with graded internal porosity. The formulations for producing these monolithic refractories were optimized for particle packing and hence permeability, using particle size distribution models.

3.2 Scaleup, Testing, and Characterization

3.2.1 Scaleup and Manufacturability Issues

ORNL, UMR, and Pyroteck closely collaborated on tasks throughout the execution of the project to ensure that any materials and processes that were developed would be inherently manufacturable, preserving as much as possible the standard practices of the refractories industry. Cost considerations were a key driver, since the refractories to be developed had to be cost effective or they would not be adopted by industrial users.

3.2.2 In-Plant Trials and Validation Testing

The autogenous coatings were evaluated in a foundry stalk/riser tube application. Figure 3.1 shows a schematic of the pressurized system used in LPD processes where the riser tubes were tested. Advanced coatings as well as monolithic castables were also evaluated for this application.

3.2.3 Wetting of Coated- and Monolithic-Refractories

As mentioned previously, it was desirable that the surface of the refractories not be wetted by molten aluminum. It is very well known that the tendencies for wetting, nonwetting, and spreading can be readily studied under carefully controlled conditions in the laboratory on the basis of the configuration of a steady-state drop of liquid (in this case aluminum) on a flat surface of the

refractory, in the so-called sessile drop test. In a joining process (brazing or soldering) it is highly desirable that the drop of molten metal wet and spread on the substrate. In the case of refractories, a nonwetting condition is desirable to prevent the formation of an intimate interface at grain boundary irregularities, and thus inhibit capillary behavior and prevent the penetration of the liquid into the refractory. Because of the importance of understanding the wetting behavior in our application, we performed the sessile drop tests with typical aluminum casting alloys on the existing refractory material as well as on newly developed monoliths with controlled porosity and optimized particle packing. In addition to measuring the wetting angles as a function of alloy and substrate composition, and process variables such as time and temperature, we characterized the interfacial composition using the microscopic characterization techniques discussed below.

3.2.4 Microscopic Characterization

As pointed out in ref. [1], a crucial part of any materials development program should be postmortem analyses of end-of-life materials. It is only through careful examination of the microstructural changes that we can develop a thorough understanding of the mechanisms of aging and progressive damage. This information can then guide the iterative process of continuous materials improvement.

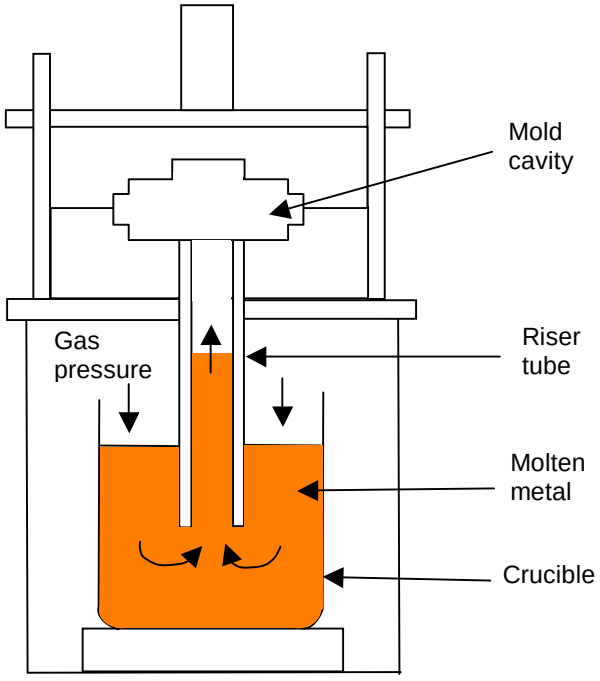

Fig. 3.1. Schematic showing utilization of riser tube during low-pressure die-casting process.

As is the case with many advanced materials, the key to the performance of these new refractory components is the interface between the bulk material(s) and the coating(s), which in this case may be of either a similar or dissimilar composition. The microstructural elements of the densified materials, both as fabricated and following exposure testing, were characterized at ORNL's microscopy facilities. Phase distributions in the interfacial region were mapped using low-voltage energy-dispersive X-ray (EDX) spectrum imaging with an analytical scanning electron microscope (SEM).

3.3 Work Breakdown Structure

The following tasks were accomplished to meet the overall objective of the proposed research and development.

3.3.1 Task 1: Characterization of DFS refractories

The focus of task 1 was to perform initial characterization of the DFS riser tubes (both as-fired and failed in service) supplied by Pyrotek**.** This involved the following steps:

1. Characterizing silica refectories by studying microstructure, macrostructure, and functional properties such as permeability and wetting characteristics with respect to molten aluminum
2. Performance of postmortem analysis of riser tubes that were in-service and experienced failure after being attacked by molten aluminum to understand the aluminum reaction kinetics

3.3.2 Task 2: Autogenous Coatings

Task 2 involved developing surface treatments to seal the surface of porous fused silica refractories to maintain the low-pressure requirements during casting operations. The research team at ORNL led on this task, while Pyrotek supplied the refractories. The surfaces of the DFS coupons were melted by exposing the coupons to a narrow band of high-density infrared (IR) energy, which after rapid solidification would form a nonporous, gas-tight barrier. The coatings were evaluated for morphology and degree of adhesion by performing metallography, and for integrity by performing a gas permeability test. The following subtasks were performed:

1. Determining cost-effective methods for surface treatment of Pyrotek refractories
2. Processing test coupons machined from Pyrotek-supplied refractory material using the high-density infrared (HID) heating system
3. Evaluating the microstructure, macrostructure, and functional properties of processed samples

3.3.3 Task 3: Advanced Ceramic Coatings

In task 3 we developed mixed-oxide coatings to seal the surface of porous fused silica refractories. The basic idea was to form a ceramic coating on the surface of the refractories by in situ reaction of the appropriate precursors, thereby taking advantage of a transient liquid phase sintering process. The following subtasks were performed:

1. Determination of coating formulations
2. Application of coatings to Pyrotek's silica refractories using various techniques such as spraying, dipping, etc.
3. Sintering coatings using a resistance furnace and/or HID heating
4. Evaluating the microstructure, macrostructure, and functional properties of coated samples

3.3.4 Task 4: Advanced Monolithic Refractories

Task 4 developed a castable refractory formulation consisting of a non-wetting system and designed with optimum particle packing to minimize the permeability of the refractory body. This task involved the following subtasks:

1. Selection of appropriate compositions for casting advanced monolithic refractories on the basis of chemical compatibility, functional properties, and cost
2. Development of a testing rig to measure the permeability of full-scale refractory components
3. Development of a particle size distribution model for optimum particle packing to minimize permeability
4. Fabrication of test coupons based on the particle size distribution model
5. Testing of coupons for behavior under thermal shock conditions as well as exposure to molten aluminum

3.3.5 Task 5: Coat and Field Test Prototype Components

In the final task ORNL and UMR assisted Pyrotek in the scaling-up of the coating techniques and fabrication of monolithic refractory components developed under laboratory conditions. The coated prototype riser tubes as well as the monolithic refractory components were to be field tested by Pyrotek at a commercial aluminum casting shop. The following subtasks were completed:

1. ORNL assisted Pyrotek in the scaling-up of the previously developed coating processes.
2. Pyrotek performed sintering of coatings on selected components using resistance furnace heating.
3. Pyrotek performed field testing of coated components at a commercial aluminum casting shop.
4. Full-scale monolithic refractories based on the formulations developed at UMR were produced at Pyrotek.
5. Pyrotek conducted field testing of refractory components at a commercial aluminum casting shop.

4. Results and Discussion

4.1 Characterization of DFS Refractories

4.1.1 Microstructural Characterization

Microstructural characterization of the as-received riser tubes from Pyrotek was performed at ORNL. One of Pyrotek's fused silica riser tubes was sectioned as shown in Fig. 4.1 to evaluate the microstructure along the tube's length. No significant differences were found. Approximately 65% of the microstructure area consists of dense SiO_2 particles about 200 μm in length, while the remaining 35% consists of loosely packed small particles 5 μm or less in size. Several specimens were cut from the tube sections in order to perform numerous characterization and processing techniques.

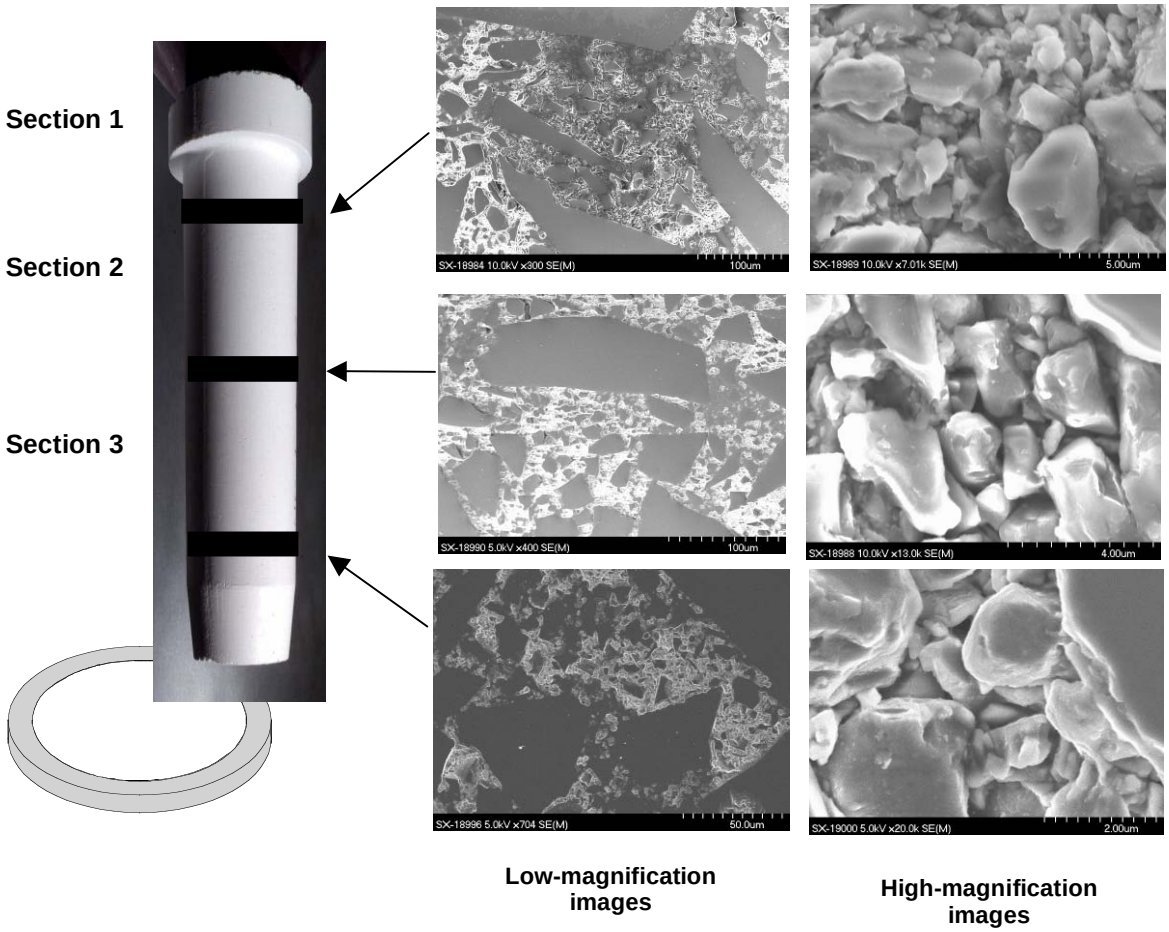

Fig. 4.1. Microstructural characterization of as-received DFS riser tube from Pyrotek.

4.1.2 Wettability and Aluminum Interaction Studies

Pyrotek supplied an original riser tube, a single-coated tube coated with boron nitride (BN), and a tube double-coated with Pyrotek's proprietary zircon-based XL glaze and BN to UMR for wettability and aluminum reactivity tests. Interactions between A356 aluminum (an Al-Si alloy) and sections of DFS riser tubes were evaluated using a sessile drop approach. Experiments were carried out in a horizontal furnace at 1225ºC under argon to minimize the effect of the aluminum oxide on the interactions at the alloy-silica interface. Images of the drop were acquired and contact angle values were measured for uncoated and coated samples, but no significant differences in the contact angles were observed. Scanning electron microscopy (SEM) revealed the presence of cracks at the interface between the reaction zone and the unreacted silica. The presence of reaction products (silicon in the reacting alloy and aluminum in a reaction zone between the alloy and the unaffected silica) has been confirmed using energy-dispersive spectroscopy (EDS). A two-layer coating system was found to be effective in reducing penetration of the aluminum alloy. Details about these studies are included in the published article reprinted in Appendix A.

In addition to these riser tubes, a used riser tube that had been reacted with molten aluminum was also sent to UMR for postmortem studies. Postmortem studies included macroscopic, microscopic, and elemental analyses of sections of reacted tube. Samples were prepared for SEM by slicing the original tube into rings approximately 1 in. thick. Each ring was then cut to size for examination by SEM. Samples were cut such that the surface along the inner diameter of the original tube that had been in contact with molten aluminum could be examined [Fig. 4.2(a)]. The samples were set in epoxy, polished, and coated with carbon. Figure 4.2(b) shows a low-magnification optical image of DFS showing non-uniform reaction across its inner diameter. The image clearly shows that the DFS tube reacted only at specific sites along the metal-tube interface. Less than half of the total inner surface of the tube showed signs of reaction. From the points of reaction, the reaction zones grew into the tube forming semispherical-shaped reactive zones. The microstructures of both the reacted and the unreacted regions in the tube were examined by SEM. SEM analysis (Fig. 4.3) showed that the apparent physical structure on the microscopic level had not changed by reaction. However, the SiO_2

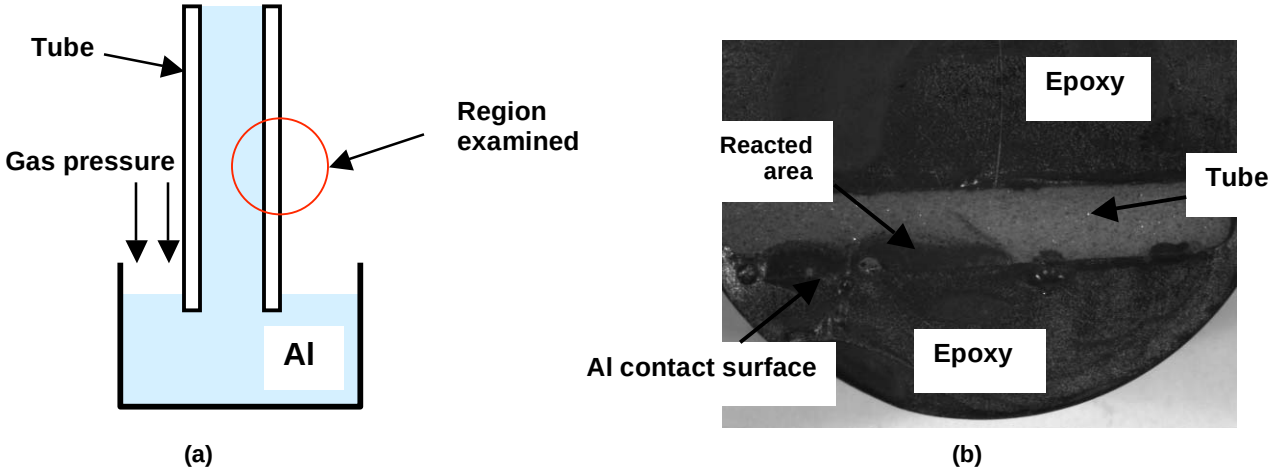

Fig. 4.2. (a) Schematic showing section of the reacted tube that was examined; (b) optical image of the dense fused silica (DFS) riser tube.

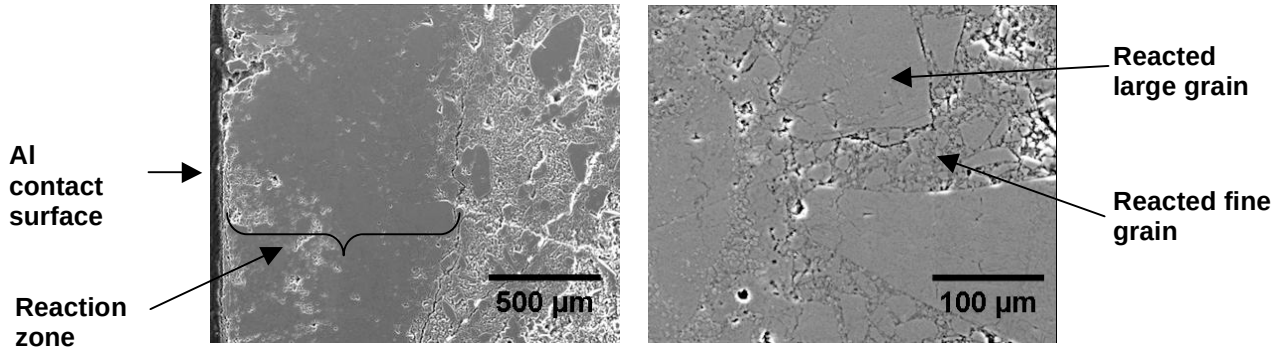

Fig. 4.3. (a) SEM micrograph showing tube section after use; (b) high-resolution micrograph of the reaction zone.

surface in the tube had been converted to Al_2O_3 and silicon in this area, as confirmed by EDS analysis (Fig. 4.4 and Table 4.1). This conversion of phases was similar to those observed in previous studies [10], where silicates and aluminosilicates have shown that they react with aluminum according to Eq. 4.1 below. EDS showed that most of the silicon was removed from the reaction zone. The oxygen was depleted in the reacted region of the tube, and aluminum was the predominant species.

$$4\ Al + 3\ SiO_2 \rightarrow 3\ Al_2O_3 + 3\ Si \qquad (4.1)$$

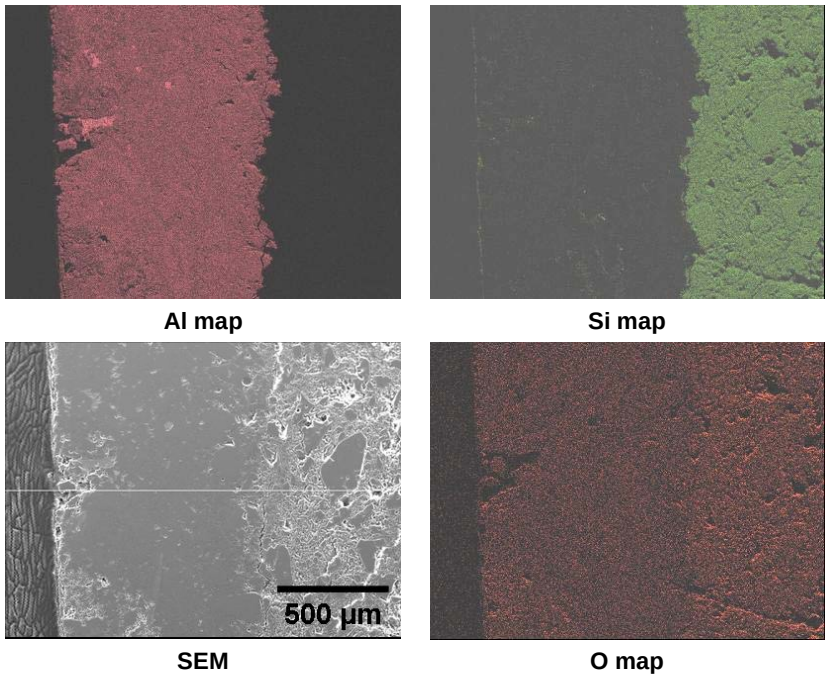

Fig. 4.4. Elemental mapping of the reacted tube section.

Table 4.1. EDS analysis of DFS tube after aluminum contact

Element	Wt %		At %		Oxide %	
	DC	UA	DC	UA	DC	UA
Aluminum	48.62	1.63	36.69	1.21	91.86	3.07
Silicon	3.39	44.68	2.46	32.00	7.25	95.59
Oxygen	47.46	52.74	60.4	66.31	—	—
All	100	100	100	100	100	100

Note: Standardless EDS results calculated using normalizing algorithms for the white tubing. Carbon excluded from analysis.

DC = discolored region; UA = unaffected region

4.2 Autogenous Coatings

Surface treatment of the wedge-shaped pieces cut from the riser tubes (shown in Fig. 4.1) was performed using ORNL's high-density infrared (IR) plasma arc lamp (Fig. 4.5). The arc lamp is a 300-kW plasma radiant source with deposition widths of 10, 20, and 35 cm and a 1-cm depth of field. The lamp is capable of delivering extremely high power densities (3.5 kW/cm^2) and has demonstrated materials-processing capabilities at temperatures in excess of 3,020°C [11]. The lamp is typically configured with a reflector to produce a line focus or an area of uniform irradiance and can be operated in either a pulse or a scan mode. Initially, the IR lamp was used to process three fused silica samples. The IR settings used for processing these three samples are shown in Table 4.2.

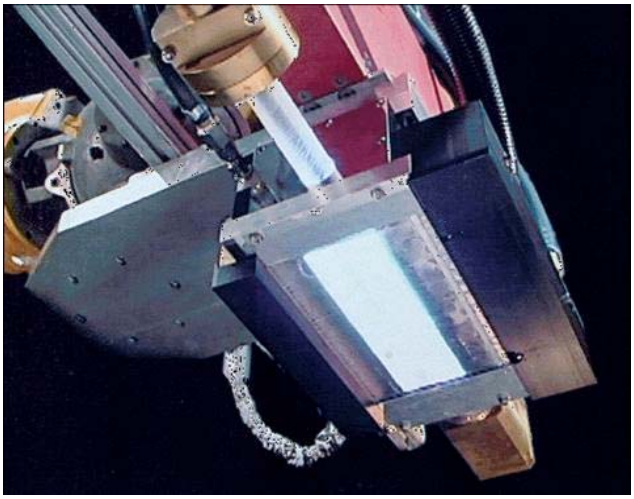

Fig. 4.5. High-density plasma arc lamp facility at ORNL.

Table 4.2. IR processing conditions

Specimen	Sample	IR amperage (A)	IR exposure time (s)	Energy input (J)
1	Fused silica	900	2	20,800
2	Fused silica	900	5	40,000
3	Fused silica	900	10	104,000

Figure 4.6 clearly shows that IR heating melted the surface of the fused silica. X-ray results (Fig. 4.7) showed that in spite of the melting, the modified or the treated surface maintained an amorphous structure similar to the one in the as-received or untreated fused silica. Observation of the cross sections of these three samples revealed increases in the depth of the melted zone with increasing exposure time. Figure 4.8 shows the variation of melt depth with increasing energy input. From the figure, one can say that it is possible to tailor the uniformity of the melt zone depths by decreasing the lamp amperage and increasing the exposure time. Thus, while it is possible to melt the entire cross section of the sample by changing the IR lamp settings, it was first necessary to evaluate the reactivity of the IR-treated surface with molten aluminum.

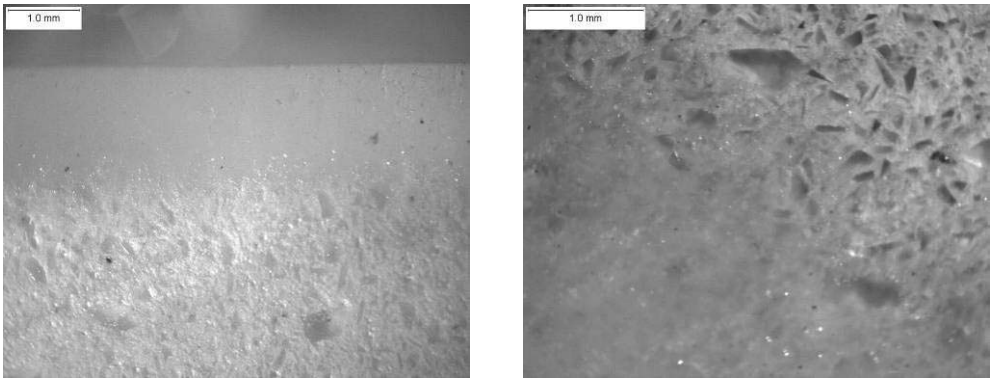

(a) **(b)**

Fig. 4.6. IR-treated fused silica: (a) side view after energy input of 104,000 joules; (b) top view after energy input of 40,000 joules.

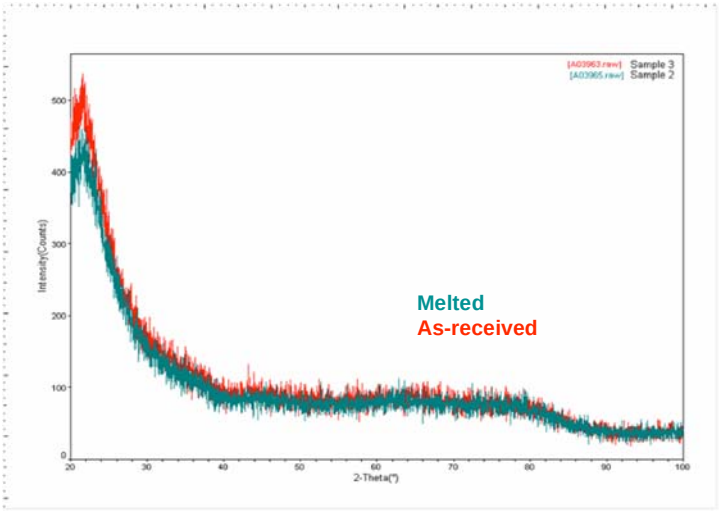

Fig. 4.7. X-ray results showing that amorphous structure of fused silica was maintained after IR heating.

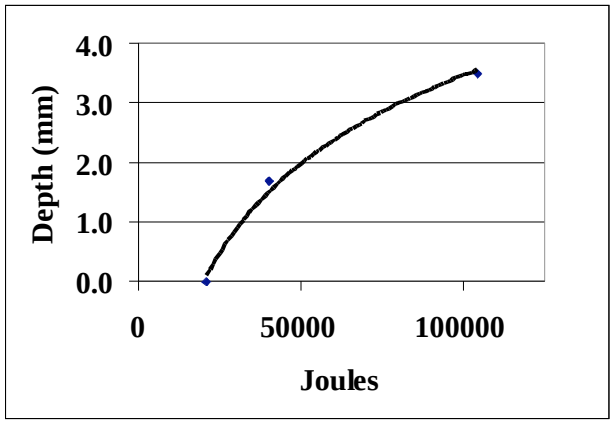

Joules	Melt zone depth (mm)
20,800	0.01
40,000	1.7
104,000	3.5

Fig. 4.8. Variation in melted zone depth with increasing exposure time.

In order to test the reactivity of the modified fused silica surface with aluminum, a small aluminum pellet was placed on the IR-treated surface of fused silica and heated to 700°C in an argon atmosphere for 30 min. For comparison, an untreated (as-received) sample of fused silica was placed with the aluminum pellet in the same furnace. After the treatment, aluminum was observed to adhere to the IR-treated surface but not to the untreated surface. It is likely that the dense structure of the treated surface may have allowed the reaction to occur faster than did the porous structure of the untreated fused silica. Pyrotek suggested that applying a nonwetting agent to the melted surface after IR treatment may prevent its reaction with aluminum. Although treatment with the plasma arc lamp showed some promise in producing a nonpermeable surface, the overall process was not effective in terms of cost and hence was not pursued further.

4.3 Advanced Ceramic Coatings

Through a literature search, several semi-crystalline (glass-ceramic) glaze compositions [12–15] were identified as potential coating materials for application on the fused silica riser tubes. The main issue in selecting the right glazes is the requirement of a low (or negative) coefficient of thermal expansion (CTE). The CTE of fused silica is 0.5×10^{-6}/°C; hence, it is very important to find a glaze material with a CTE value that is even lower, to prevent cracking or spalling of the coating. Semi-crystalline glazes have been proven to have the right combination of lower CTE crystalline phases dispersed in a glassy matrix, making it possible for them to have an overall lower CTE value. The CTE values of semi-crystalline glazes can be tailored depending on the crystalline phases and the content of the glassy phase present. Table 4.3 lists some of the glaze compositions discussed in the literature with CTE values that closely match that of fused silica.

Of the several glaze compositions, the oxide mixtures numbered 1, 6, 7, and 8 were selected because of their lower CTE values, and 100 g of each glaze mixture containing the respective weight percentages of the individual oxides was prepared. Each mixture was dry-milled for 25 min and then wet-milled for 2 h with ethanol to form slurries. Several wedge-shaped pieces were sectioned from the riser tube (as shown in Figure 4.1) and oven-dried at 350°C for 3 h. The preheating/drying was carried out to remove any volatiles or moisture that had become entrapped during or after the manufacturing of the riser tubes. The dried wedge-shaped pieces were dipped in the four slurries corresponding to glaze mixtures 1, 6, 7, and 8, as shown in Table 4.3. The firing schedule used to develop the desirable crystalline phases within the four glazes is shown in Table 4.4. The glazes were fired in an electric resistance-heated box furnace (Micropyretics Heaters International).

Table 4.3. Oxide composition (wt %) of selected glazes with low coefficients of thermal expansion (CTEs)

Oxide component	Glaze							
	1[a]	2[a]	3[b]	4[c]	5[c]	6[d]	7[e]	8[e]
Al_2O_3	29.2	27	26.98	26.04	21.67	23.19	11.29	14.79
B_2O_3	5	—	4.98	2.65	1.96	—	—	—
CaO	—	—	—	—	—	3.05	4.56	5.96
K_2O	5	5	5.05	4.41	3.83	—	—	—
Li_2O	11.3	9	9.08	9.35	7.75	4.53	3.31	4.34
MgO	—	—	—	—	—	6.58	3.27	4.28
SiO_2	49.5	54	53.91	55.33	51.06	62.65	47.48	53.83
ZnO	—	—	—	—	1.02	—	30.9	16
ZrO_2	—	5	—	2.21	12.71	—	—	—
CTE	**–0.9**	**1.9**	**NR**	**NR**	**NR**	**1.3**	**0.34**	**0.36**

[a]Semicrystalline glazes for low-expansion whiteware bodies
[b]Ceramic solutions
[c]Glazes and glass coatings
[d]Thermal expansion data of some alkali aluminosilicate glasses and their respective glass-ceramics
[e]Crystallization of some aluminosilicate glasses
NR = not reported

Table 4.4. Firing schedule for various glaze compositions

Glaze	Firing schedule (°C/h)	Heat treatment schedule (°C/h)	Heating rate (°C/min)	Phases expected[a]	ΔGrxn (kJ @ 700°C)
1	1094/0.25	—	20	β-spodumene ss	–142
	788/0.50	—	20		
6	1500/4	850/5	3	β-spodumene ss,	–142
		1050/3	3	β-eucryptite ss, clinopyroxene	–72 —
7	1450/3.5	660/4	3	β-spodumene ss,	–142
		900/3	3	β-eucryptite ss, Willemite	–72 –416
8	1450/3	660/4	3	β-eucryptite ss,	–72
		780/3	3	Willemite, Diopside	–416 —

[a]The following are crystalline phases: β-spodumene solid solution ($LiAlSi_2O_6$), β-eucryptite solid solution ($LiAlSiO_4$), clinopyroxene ($MgSiO_3$ + $CaMgSi_2O_6$), Willemite (Zn_2SiO_4) and Diopside ($CaMgSi_2O_6$).

The free energy of reaction between fused silica and molten aluminum at 700°C was estimated to be –503.1 kJ [10]. Since the free energies of reaction between the crystalline phases and molten aluminum are higher than –503.1 kJ, the probability of the glazes reacting with molten aluminum is less thermodynamically favorable than the reaction with silica. Figure 4.9 shows optical micrographs of the cross-sections along the glaze/fused silica substrate interface. All glazes appear to be continuous and show good bonding with fused silica, except for some porosity within the glaze representing glaze 1 composition. High-magnification SEM micrographs of the glaze sections and fused silica substrates (Fig. 4.10) after the firing process show a crystalline phase–like structure within the glazes and a modified substrate structure for all glazes, except for glaze corresponding to glaze 1. The altered structures within the glazes and the substrate were also verified by performing X-ray diffraction analysis. Figures 4.11, 4.12, and 4.13 show the diffraction patterns corresponding to the various glazes and fused silica substrates. X-ray results for the glazes show the presence of various crystalline phases as expected (see Table 4.4). However, X-ray results from the substrates show formation of crystalline cristobalite in cases where the firing temperatures were above 1200°C (i.e., the firing schedule for glazes corresponding to compositions 6, 7, and 8). The presence of crystalline cristobalite can lead to severe cracking of the riser tube and can also increase its reactivity with molten aluminum, and is therefore highly undesirable. Based on the X-ray results and the free

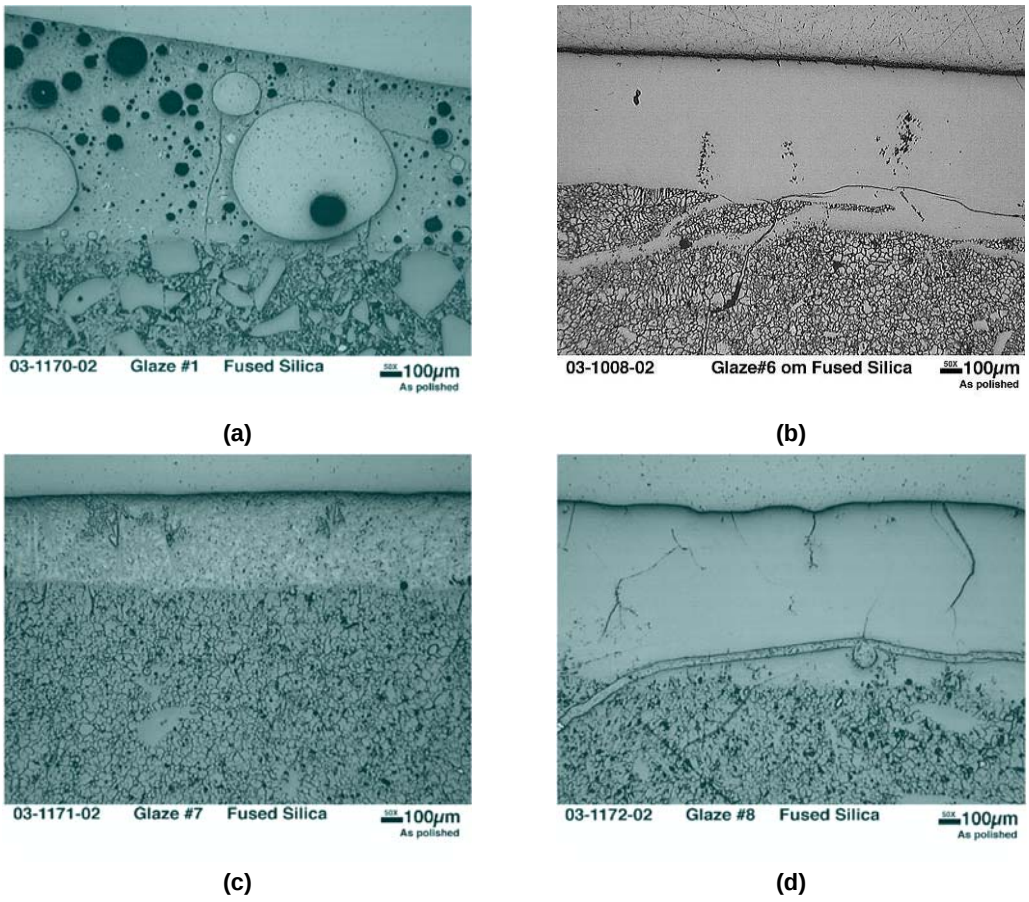

Fig. 4.9. Optical micrographs showing cross sections along the glaze/substrate interface corresponding to (a) glaze 1, (b) glaze 6, (c) glaze 7, and (d) glaze 8 compositions.

energies of reaction between the various crystalline phases and aluminum at different temperatures (Table 4.5), it was concluded that of the four glazes, the composition as well as the thermal cycle corresponding to glaze 1 is capable of producing the desired crystalline phases without altering the substrate and hence could be considered as a suitable candidate for scaleup.

Table 4.5. Free energy of reaction of various crystalline phases

Temperature (°C)	$\Delta G_{reaction}$ of various crystalline phases with aluminum (kJ)		
	$LiAl_2SiO_6$	$LiAlSiO_4$	Zn_2SiO_4
527	–152.8	–80.8	–420.7[a]
627	–148.1	–76.5	–419.1
727	–142.1	–71.2	–415.9

[a] At 727°C, Zn_2SiO_4 is highly reactive with aluminum and should be avoided in the glaze.

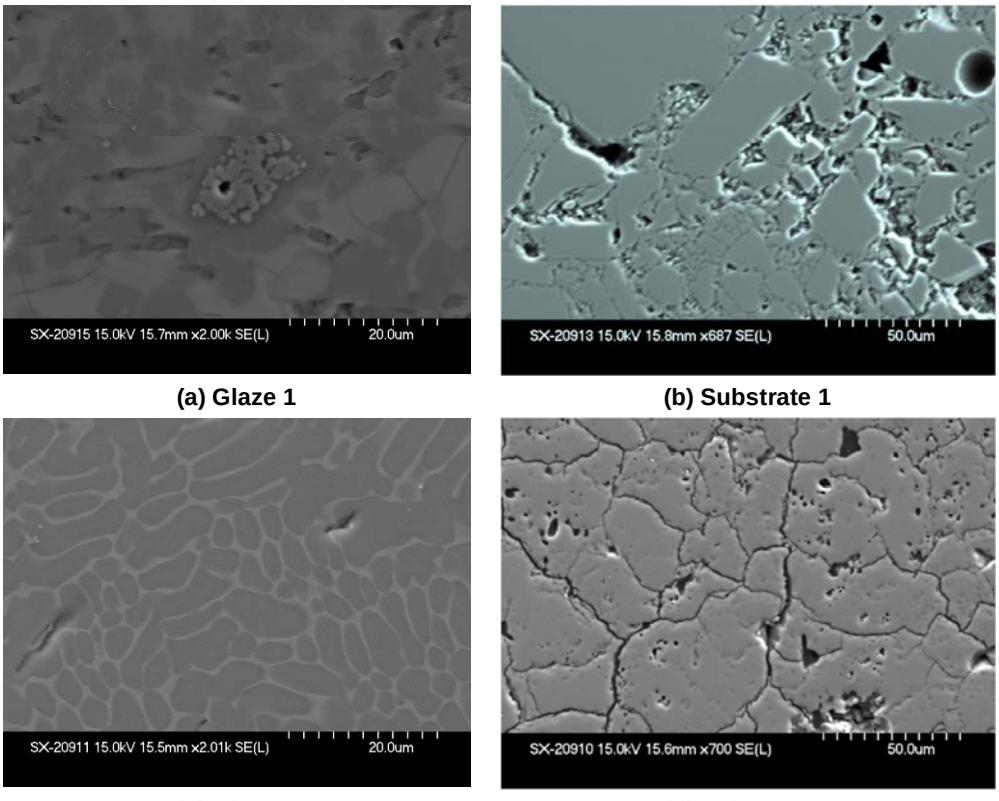

(a) Glaze 1 **(b) Substrate 1**

(c) Glaze 6 **(d) Substrate 6**

Fig. 4.10. SEM micrographs showing glaze section and fused silica substrate after the firing process.

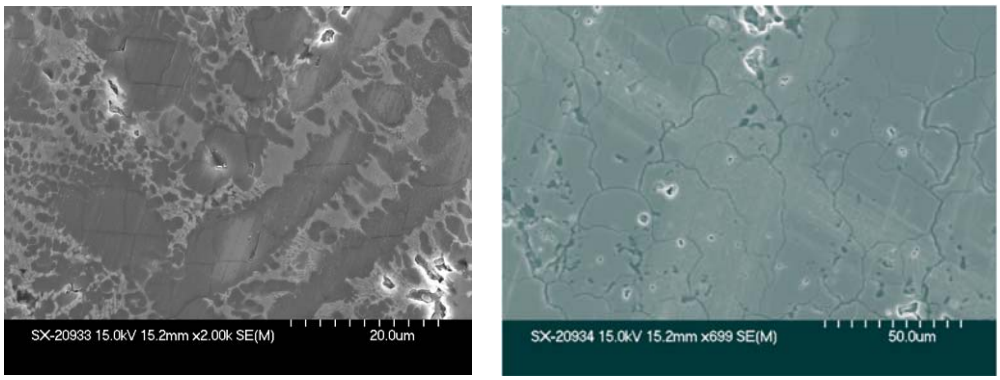

(e) Glaze 7 **(f) Substrate 7**

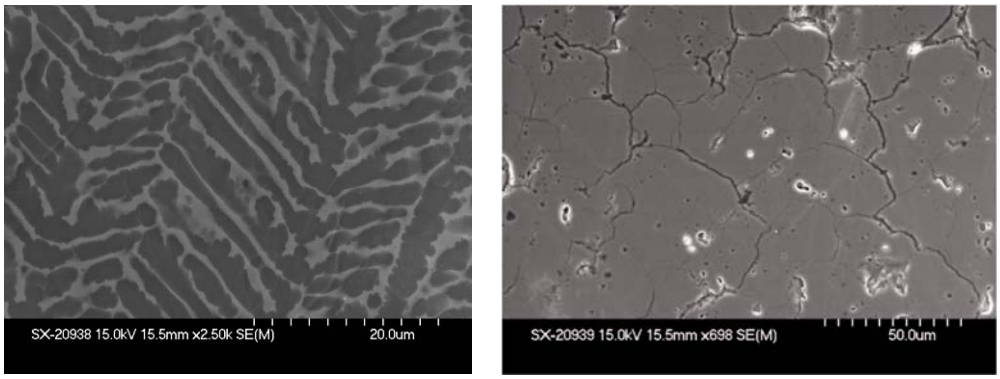

(g) Glaze 8 **(h) Substrate 8**

Fig. 4.10 (cont.). SEM micrographs showing glaze section and fused silica substrate after the firing process.

Although the preliminary results showed that glaze 1 was an appropriate glaze material, additional studies such as measurement of CTE values, bonding characteristics at elevated temperature and under thermal cycling (thermal fatigue), and reactivity and wettability with molten aluminum were necessary before the glaze could be considered for full-scale application.

CTE measurements of the monolithic glaze 1 material was performed with a dual push rod dilatometer. Monolithic samples of glaze 1 were prepared by simply firing the glaze mixture in a porous alumina crucible and then machining the specimen directly out of the crucible. During CTE measurement, the sample was heated up to 700°C at 10°C/min and then allowed to cool to room temperature. The sample was subjected to two such heating and cooling cycles. During the heating and cooling cycle, the change in the length of the specimen with temperature was measured in relation to the change in the length of the standard reference specimen. The mean CTE was calculated as change in length over a specific temperature range $(\Delta L/L_0)/(T–20°C)$. Figure 4.14 shows the change in the expansion and mean CTE values for the glaze 1 specimen as a function of temperature. As the figure shows, glaze 1 showed negative CTE values at lower temperatures (below 315°C); at higher temperatures, however, the values were positive and an order of magnitude higher than the values for fused silica. The mean CTE values during the second heating and the cooling cycle were always positive, and the specimen was observed to have been permanently strained. The change in the mean CTE values during the second cycle could be due to phase change or change in the amount of

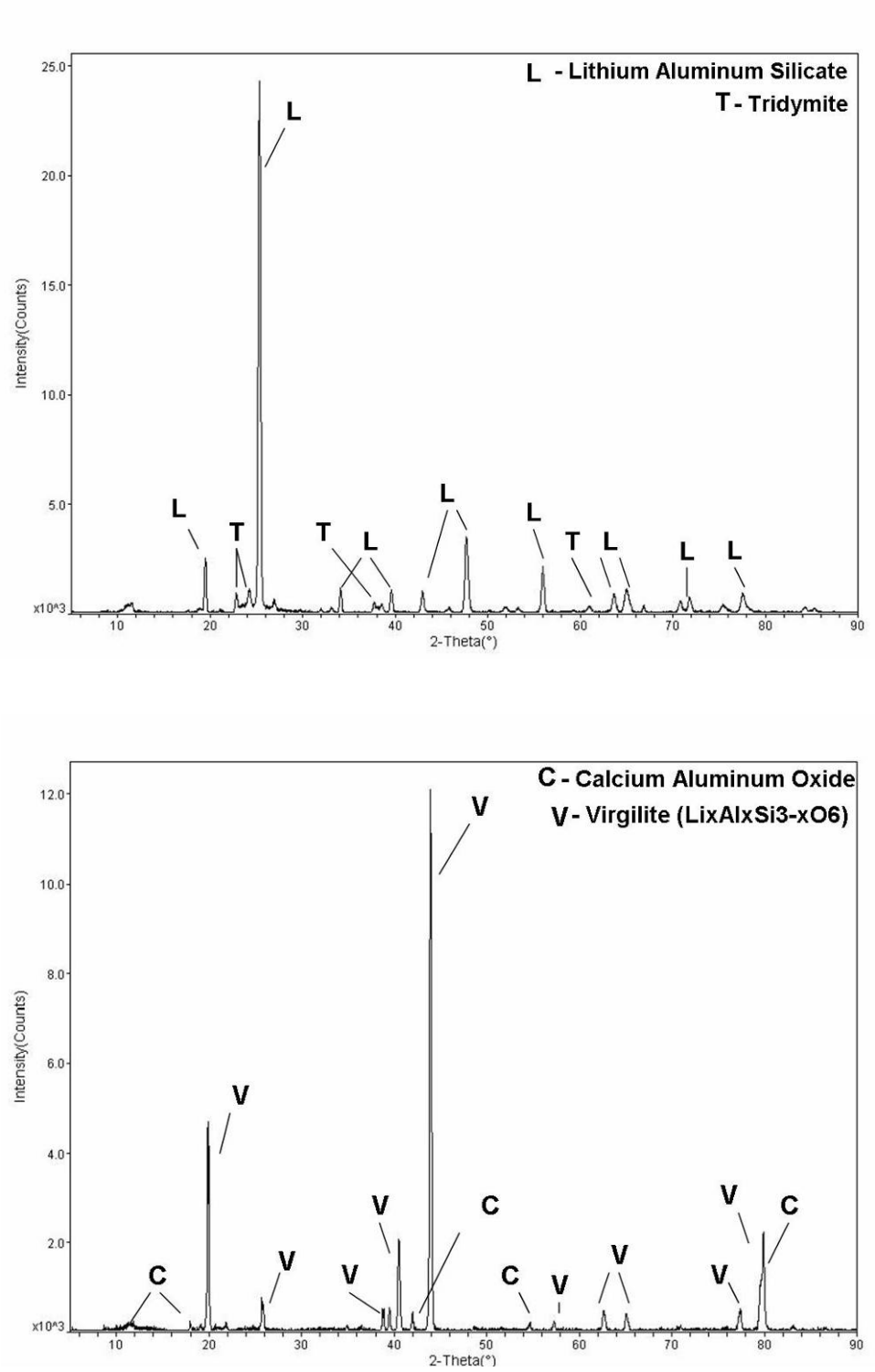

Fig. 4.11. X-ray diffraction pattern showing various crystalline phases formed within the glaze after the firing process: *top,* glaze 1; *bottom,* glaze 6.

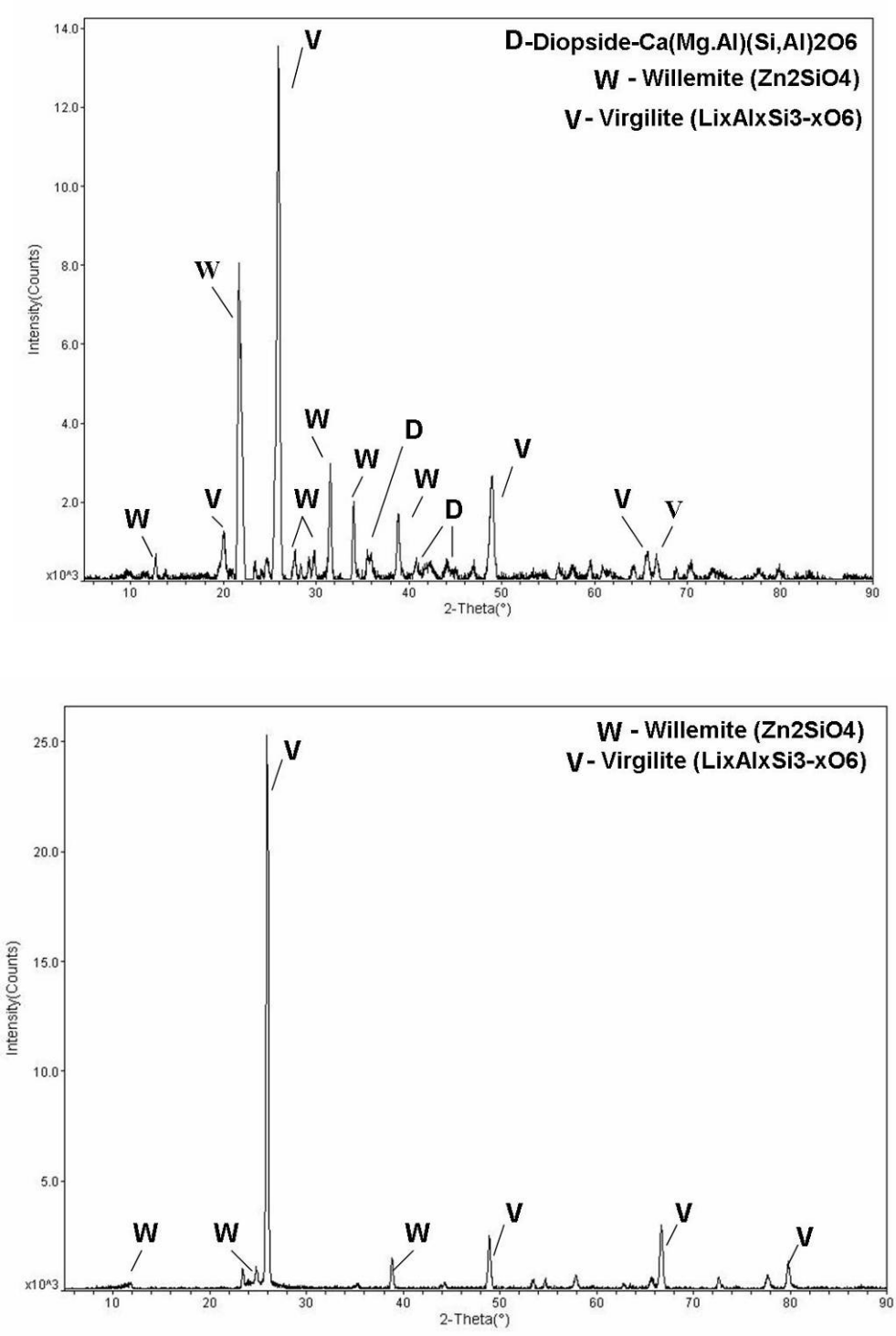

Fig. 4.12. X-ray diffraction pattern showing various crystalline phases formed within the glaze after the firing process: *top,* glaze 7; *bottom*, glaze 8.

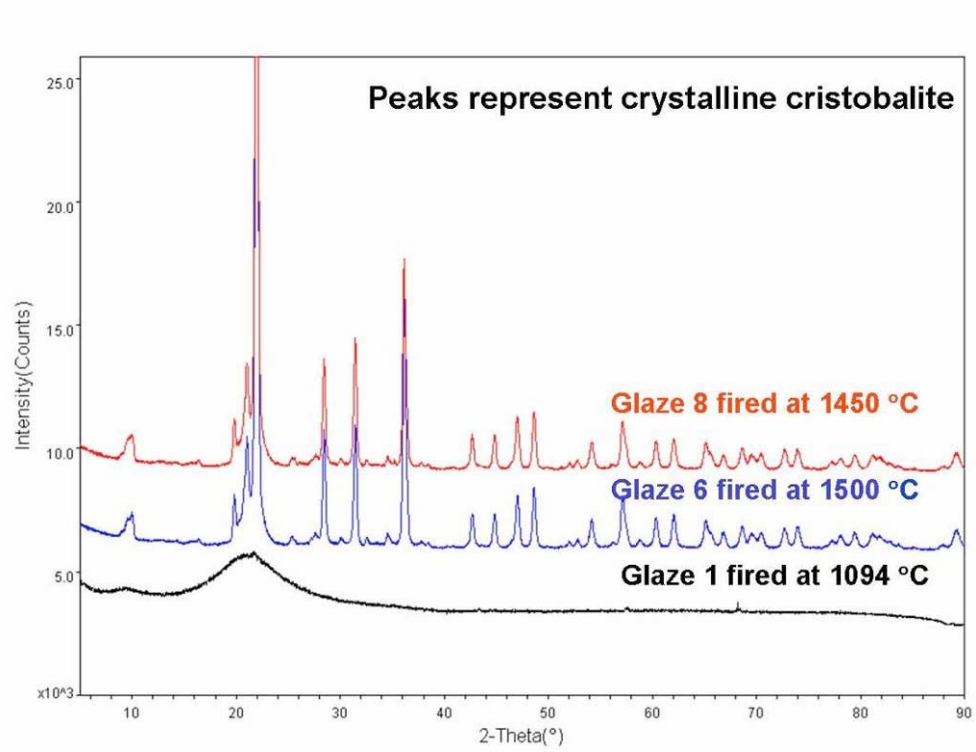

Fig. 4.13. X-ray diffraction pattern showing cristobalite formation in fused silica substrate after firing of glazes 6 and 8 at temperatures above 1200°C.

crystallinity occurring during the first heating cycle when the sample reached 700°C. X-ray analysis of the specimen before and after the CTE measurement was performed to find out what changes in the amount of crystallinity and in the formation of newer lithium-aluminosilicate crystalline phases with slightly different stoichiometry occurred during the heating and cooling cycles (Fig. 4.15).

While the monolithic glaze specimen was being tested for thermal cycling during CTE measurements, separate tests to study the effect of thermal cycling on the integrity and bonding characteristics of glaze 1 when applied to fused silica were performed. This study was necessary to simulate the actual conditions of alternating high and lower temperatures to which the fused silica down tube would be exposed during aluminum casting operations. For the performance of these tests, the glazed fused silica samples were heated to 700°C at 100°C/min, held at 700°C for 10 min, and then cooled to room temperature at 100°C/min. This process was repeated twice, and the samples were then inspected to see if any cracking or debonding of the glaze occurred from the heating and the cooling cycle. No spalling or cracking within the glaze layer or the fused silica substrate was observed, and X-ray results (Figure 4.15) showed that the original crystalline phases seen in glaze 1 were retained, except for a slight increase in the amount of crystallinity.

After the thermal fatigue tests, evaluation of glaze 1 was continued to understand its reactivity with molten aluminum. Three wedge-shaped pieces of fused silica glazed on only one surface were immersed in molten aluminum alloy AA356 at 750°C for 24, 48, and 72 h. Visual examination of the cross sections of these reacted fused silica pieces indicated increasing depths of aluminum penetration through the unglazed surfaces of fused silica as a function of exposure time (Fig. 4.16). Cross sections of fused silica subjected to 72 h of exposure showed aluminum penetration throughout the thickness of the sample. Optical micrographs of the glaze/molten aluminum interface showed only minimum

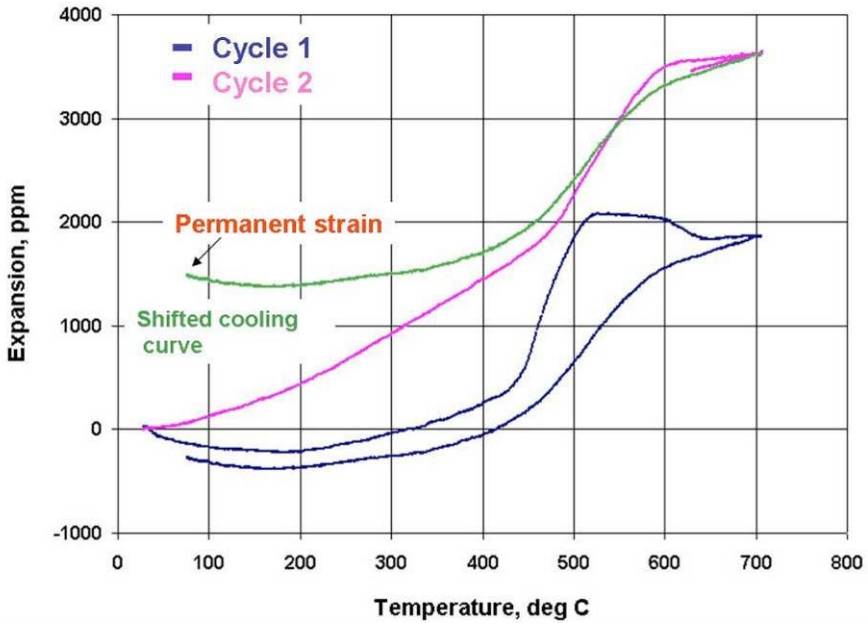

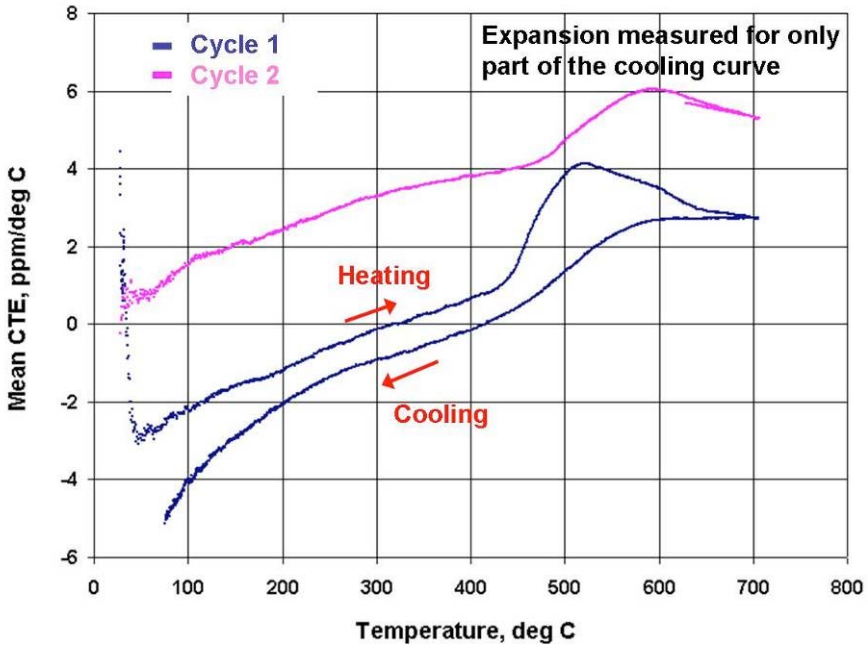

Fig. 4.14. Dilatometer test results for CTE measurements of glaze 1: (*top*) expansion of specimen; (*bottom*) mean CTE as a function of temperature.

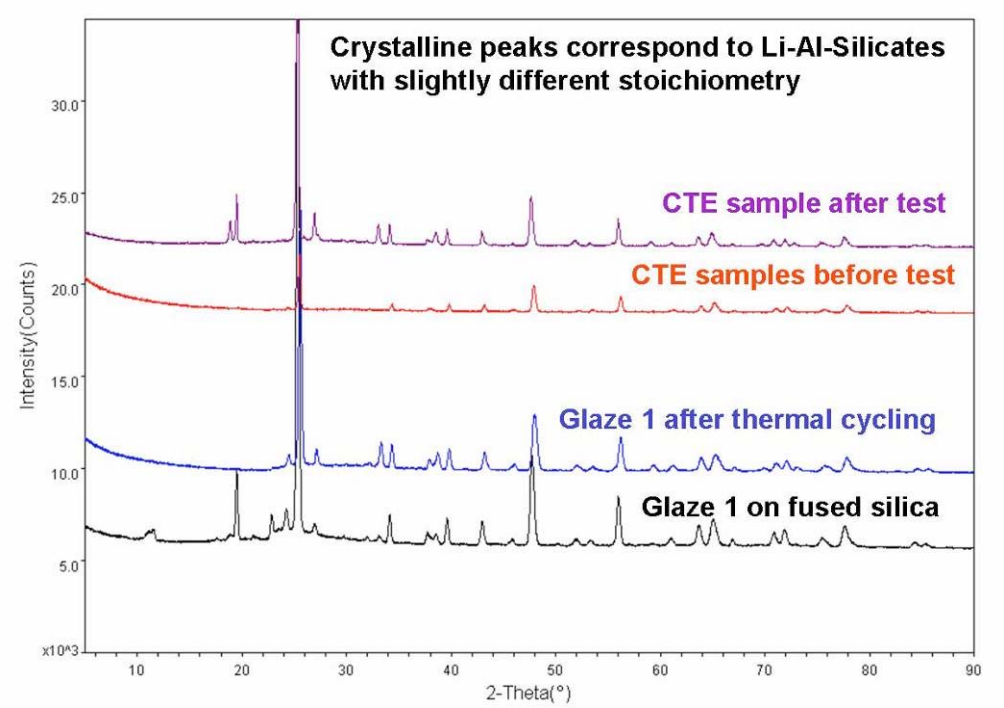

Fig. 4.15. X-ray analysis of specimen before and after CTE measurement.

As glazed (center)

Fused silica being attacked from unglazed surfaces: *left,* 24 h; *right,* 48 h

Entire cross section attacked

Fig. 4.16. Reactivity of glaze 1 with molten aluminum for different exposure times.

metal attack for both the 24-h and the 48-h exposures (Fig. 4.17); however, severe spalling, metal penetration, and cracking of the glaze was observed in the sample exposed for 72 h. We assume that porosity and other defects, such as fine cracks, within the glaze provided a pathway for the metal to penetrate through the glaze. Also, immediate attack and penetration of the metal through the unglazed surfaces of these samples is likely to hinder the actual evaluation of the glaze performance during the reactivity tests.

Although the test results for glaze 1 look promising, closing the porosity within the glaze layer is important in improving its performance, especially in preventing the metal penetration. Efforts were made to produce more glazes by altering the glaze 1 firing cycle (by using a slower heating rate and long holding times at temperature), anticipating that such changes would provide sufficient time for the volatiles (either from glaze or the substrate) to escape. However, the attempts were unsuccessful and the porosity persisted.

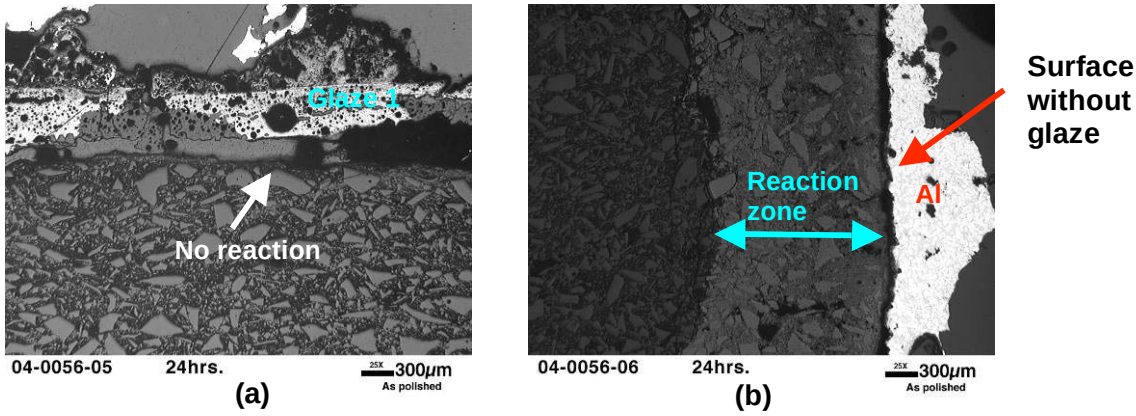

Fig. 4.17. Comparison of sample (a) with and (b) without protective glaze 1 after 24-h exposure at 750°C.

Based on thermodynamic calculations, another possibility for pore or bubble formation in glaze 1 is decomposition of lithium carbonate (Li_2CO_3) after it has melted. Li_2CO_3 acts a flux as well as a source for Li_2O in the glaze composition, and its melting temperature is 660°C. Based on the partial pressure of CO_2 in the decomposition atmosphere, the equilibrium decomposition temperatures for both solid and liquid Li_2CO_3 were calculated to be in the range of 735 to 1176°C. (The maximum firing temperature for firing glaze 1 is 1094°C.) Thus, the decomposition of Li_2CO_3 and the release of CO_2 after the Li_2CO_3 has melted may cause pore formation if the glaze is applied as an unreacted powder.

In an effort to eliminate porosity due to decomposition of Li_2CO_3 , the composition and the firing process for the glaze 1 mixture were modified using two different approaches: (1) reducing the Li_2CO_3 content in the starting glaze mixture and replacing the reduced fraction with spodumene (lithium aluminum silicate) as a source of Li_2O in the glaze composition, and (2) pre-reacting or fritting the existing glaze mixture. Fritting of the glaze mixture was carried out at UMR using a lab-based fritting furnace. During the fritting process, the mixture was heated up to 1425°C at a rate of 20°C/min and held at this temperature for 3 h. The molten mixture was quenched in cold water to form an amorphous lump of frit. The frit was crushed and then remelted twice under the same condition to ensure homogeneity. The final frit was crushed with a high-speed impact crusher to achieve a particle size of ~40 μm and later mixed with polyethylene glycol and polyvinyl alcohol to form a slurry prior to its application on fused silica. The firing schedule typical for glaze 1 was used for firing the fritted glaze. Figure 4.18 shows the micrographs of glaze 1 with reduced Li_2CO_3 and containing spodumene, and with the fritted glaze mixture. Micrographs show a strongly fused coating for the two conditions, with some reduced porosity in the former case; however, porosity was still present.

4.4 Advanced Monolithic Refractories

4.4.1 Permeability of Dense Fused Silica

For measurement of permeability in DFS refractories, an apparatus based on the vacuum-decay permeametry method [16] was developed at UMR. With this method, the porous sample is placed between two chambers and subjected to a transient pressure gradient. Figure 4.19 shows a schematic of the permeameter. A porous disc (a DFS discs in this case) 2 in. in diameter and 1 in. thick is fixed

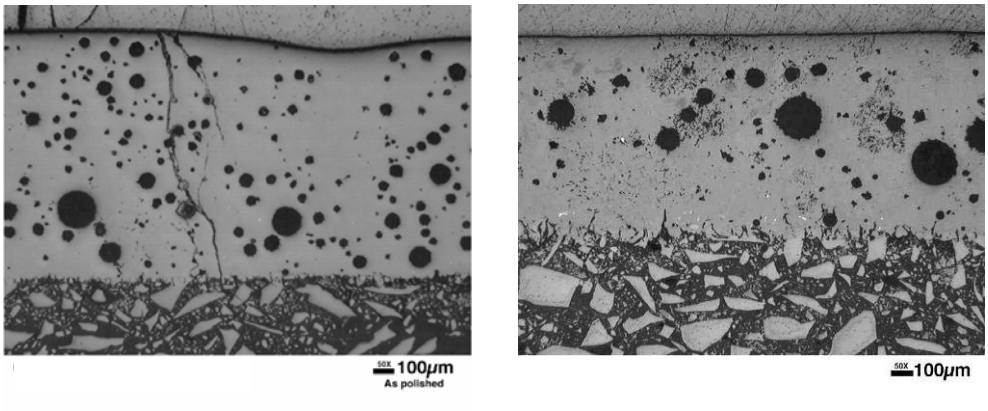

(a) (b)

Fig. 4.18. Micrographs of glaze 1 on fused silica (a) with reduced Li_2CO_3 and containing spodumene in the glaze mixture and (b) with the fritted glaze mixture.

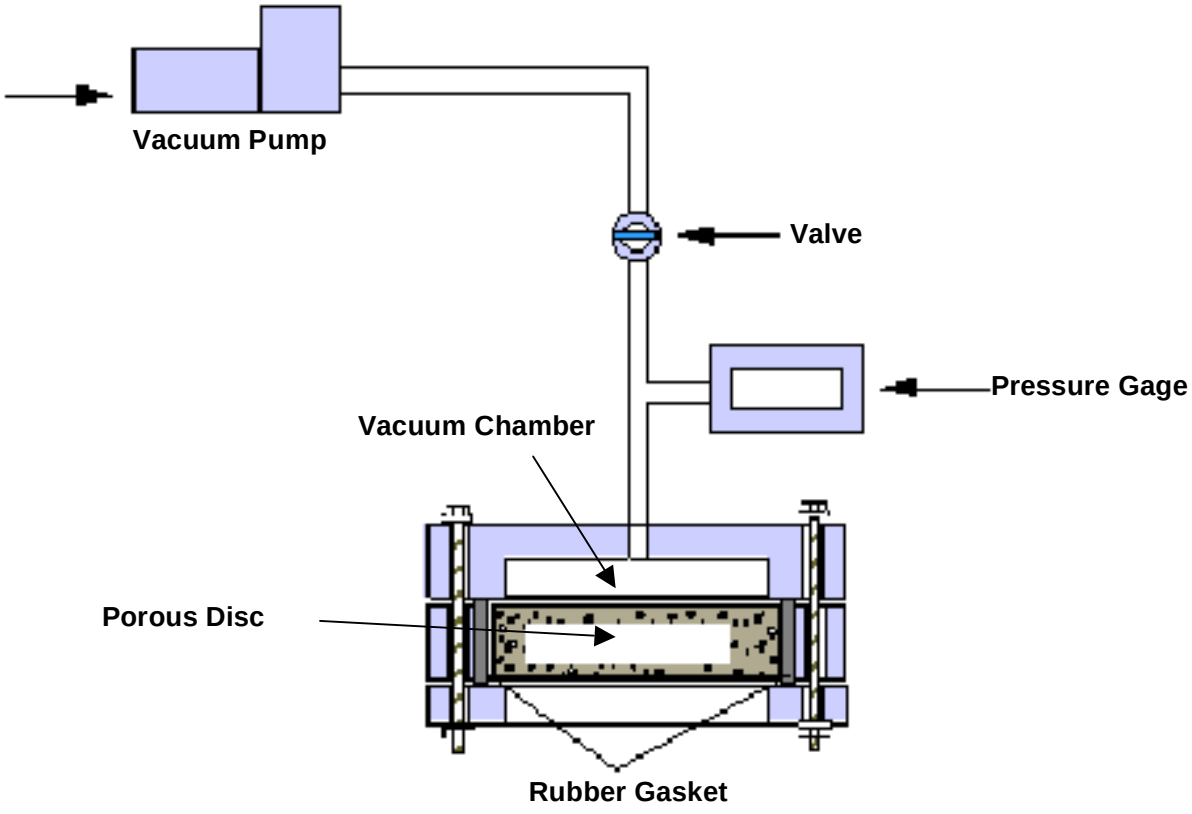

Fig. 4.19. Schematic of the vacuum-decay permeameter.

between a vacuum chamber on one side and another chamber at atmospheric pressure on the other side. As the air flows from the atmosphere to the evacuated chamber through the porous disc, a vacuum-decay or a pressure decay-curve is recorded with respect to time (Fig. 4.20). The permeability constant (K in mDarcy) is calculated by applying Darcy's law to the pressure-decay curve and using Eq. (4.2), where Q is determined from dP/dt and system volume:

$$K = \frac{\eta Q L}{A \Delta P}, \tag{4.2}$$

where

η = fluid viscosity in cP
Q = volumetric flow rate in cm^3/s
L = sample length in cm
A = sample area in cm^2
ΔP = absolute pressure drop across the sample in atm

In the case of a DFS tube, the above formula can be modified as Eq. (4.3):

$$K = \frac{\eta \ln\left(R_o / R_i\right) Q}{2\pi L \Delta P}, \tag{4.3}$$

where R_O and R_i are tube outer and inner radii in cm, respectively; L is the tube length in cm; and ΔP is the differential pressure across tube wall in atm. Figure 4.21 shows a pemeameter developed to measure the permeability of a full-scale DFS tube. The test fixture can accommodate tubes with varying diameters and lengths.

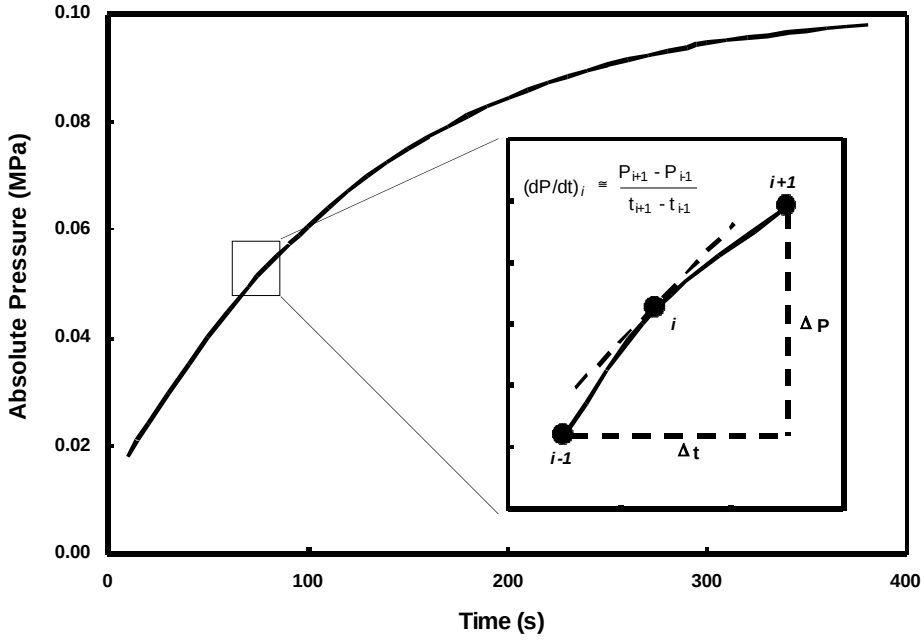

Fig. 4.20. Typical pressure decay curve recorded during permeability measurement.

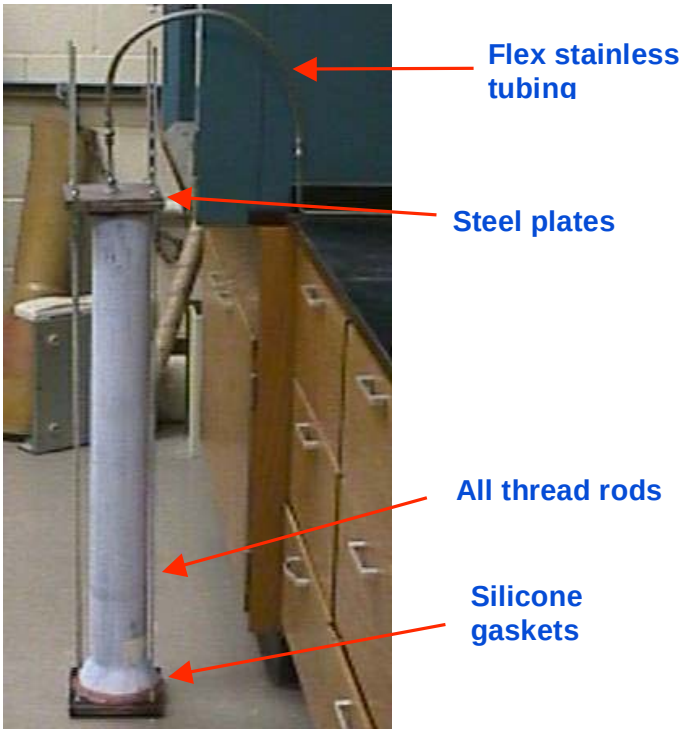

Fig. 4.21. Full-scale permeameter developed at UMR.

A number of tests were performed using this full-scale setup to identify the right gasket material for room-temperature and high-temperature testing, to ensure proper fastening between the swage lock and stainless piping seals, and to verify the reproducibility of the pressure decay. Figure 4.22 shows the results of reproducibility tests performed on a single DFS tube using the full-scale permeameter.

4.4.2 Optimization of Particle Packing Density for Minimum Permeability

New formulations for fused silica castable tubes were developed at UMR based on the optimized packing of different particle sizes using a continuous distribution. A three-parameter continuous distribution model based on the Funk and Dinger relationship [Eq. (4.4)] having the potential of achieving nearly full densities was used to optimize the particle packing.

$$CVPFT = \frac{D^n - D_s^n}{D_l^n - D_s^n} \tag{4.4}$$

where

n = distribution modulus
D = particle size
$CVPFT$ = cumulative vol % of particles with diameters <D (cumulative vol % finer than)
D_l = largest particle size in the distribution
D_s = smallest particle size in the distribution [17]

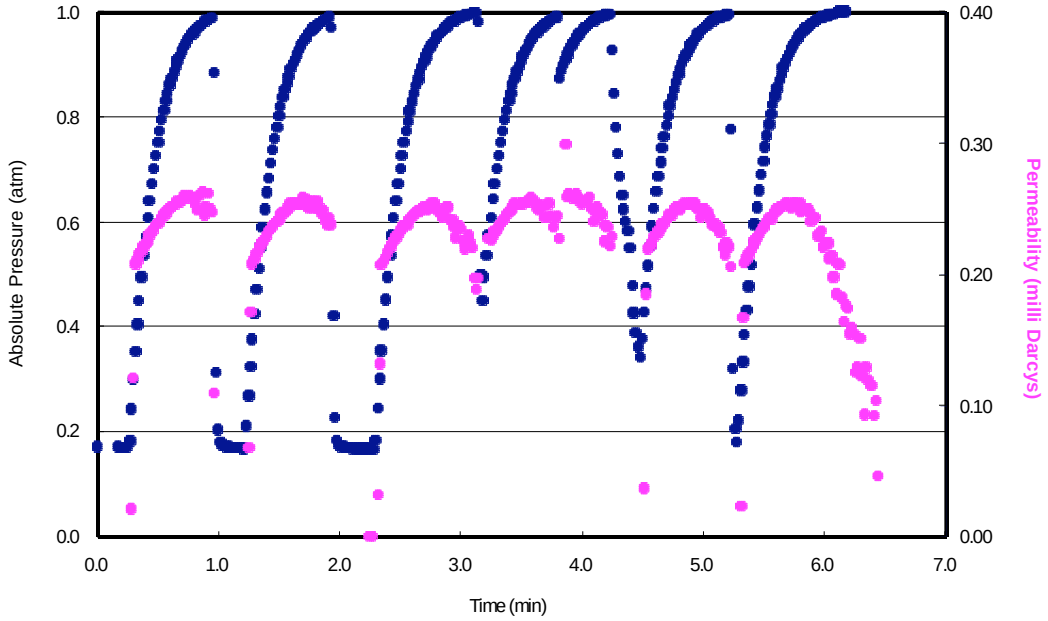

Fig. 4.22. Permeability test results showing reproducibility in pressure decay data.

A computer model based on this theory (and using particle size distributions measured for the raw materials to be used in the formulation) was developed to predict the weight percent of each raw material that should be added to the formulation to optimize the particle packing and achieve the highest density. The model (Fig. 4.23) also gives the deviation within each size class to show which particle sizes need to be added to the formulation to improve the packing density. For initial formulations, the particles were assumed to be perfect spheres. In calculations of the target formulation aimed at achieving near-theoretical bulk densities, the value of n was taken to be 0.37. Figure 4.24 represents the target and the predicted particle size distributions and deviations for the formulation shown in Table 4.6.

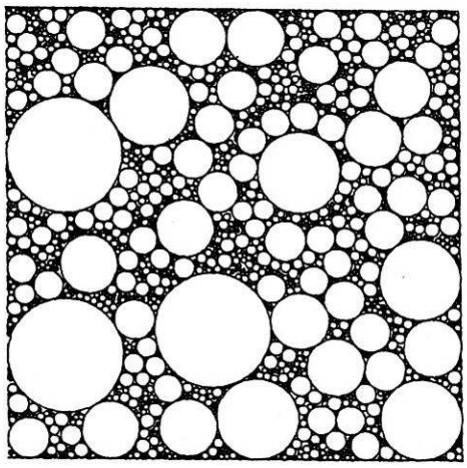

Fig. 4.23. Computer model predicting particle size distribution for optimized packing density.

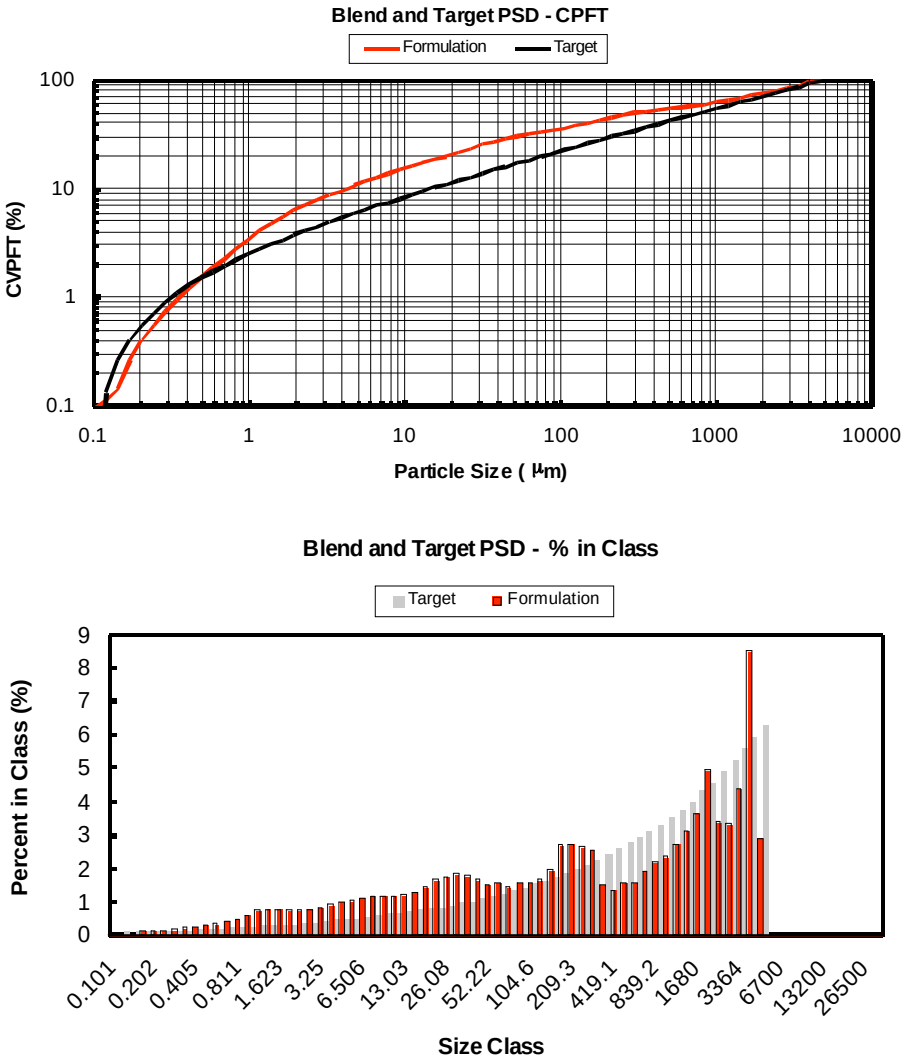

Fig. 4.24. (a) Particle size distribution (PSD) and (b) deviation within each size class for formulation shown in Table 4.6.

Table 4.6. Initial formulation based on the continuous distribution model

Component	Wt %	Vol %
Size fraction 1	25.3	28.41
Size fraction 2	11.0	12.38
Size fraction 3	7.3	8.25
Size fraction 4	7.3	8.25
Size fraction 5	8.3	6.41
Size fraction 6	8.3	6.41
Reactive alumina	7.3	6.02
Nonwetting 1	5	2.77
Nonwetting 2	5	6
Fume	8	9
Cement	7	6

Maximum Size (mm)	5600
Minimum Size (mm)	0.37
Modulus	0.20

Table 4.6 gives the weight and volume percentages of various raw materials that should be added to the formulation to achieve the optimal particle size distributions (PSDs) as shown in Fig. 4.24. The discrepancies between the target PSD and the formulation PSD were caused by factors or constraints such as water content, cement content, additive content, particle shape, etc., in the formulation that affected the packing density. Figure 4.25 show the particle size distribution and deviation within each size class when no nonwetting agents and lower cement contents were allowed in the formulation (i.e., the formulation was unconstrained). Table 4.7 represents the weight and volume percentage of the various raw materials when the formulation was unconstrained. Similar formulations and PSDs could also be achieved by constraining the formulation by including certain compounds in specific quantities and then recalculating the quantities of other compounds to achieve the targeted PSD or particle packing. Table 4.8 provides an example.

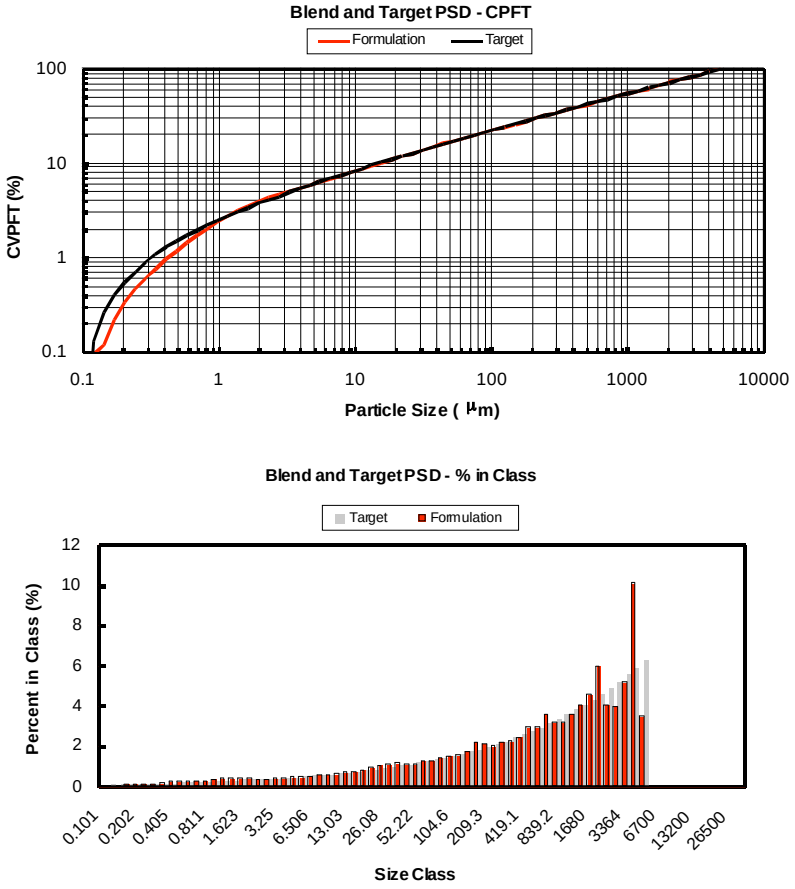

Fig. 4.25. (a) Particle size distribution (PSD) and (b) deviation within each size class for unconstrained formulation shown in Table 4.7.

Table 4.7. Unconstrained formulation for silica castables: no nonwetting agent 1 and lower cement

Component	Wt %	Vol %
Size fraction 1	31.1	33.79
Size fraction 2	14.9	16.22
Size fraction 3	14.4	15.67
Size fraction 4	5.2	5.67
Size fraction 5	8.0	5.97
Size fraction 6	9.6	7.16
Reactive alumina	6.4	5.07
Nonwetting 1	0	0
Nonwetting 2	2	2
Fume	6	6
Cement	3	2

Table 4.8. Two constrained formulations for silica castables

	Constrained formulation A[a]		Constrained formulation B[b]	
Component	Wt %	Vol %	Wt %	Vol %
Size fraction 1	30.4	33.83	30.6	33.84
Size fraction 2	14.5	16.18	14.6	16.13
Size fraction 3	14.0	15.64	14.3	15.81
Size fraction 4	5.2	5.82	3.7	4.15
Size fraction 5	7.6	5.78	12.8	9.68
Size fraction 6	10.4	7.92	4.4	3.34
Reactive alumina	3.9	3.15	2.6	2.11
Nonwetting 1	5	2.74	5	2.72
Nonwetting 2	5	5	4	5
Fume	0	0	3	3
Cement	5	4	5	4

[a]For formulation A, the constraint is 5 wt % of each of the nonwetting agents, 0 wt % of fume, and 5 wt % of cement

[b]For formulation B, the constraint is 5 wt % of nonwetting agent 1, 4–6 wt % of nonwetting agent 2, ≥3 wt % of fume, and 5 wt % of cement

4.5 Coat and Field Test Prototype Components

4.5.1 Advanced Ceramic Coatings

Based on the promising results observed at the laboratory scale, Pyrotek decided to scale up the glazing process developed at ORNL. A mixture corresponding to the composition of glaze 1 was prepared at Pyrotek using commercial-grade oxides and carbonates and using water as a solvent.

Spodumene, instead of lithium carbonate, was used as a source for lithium oxide. After the slurry was prepared, a large section of a riser tube was dipped in the slurry and then gradually pulled out to obtain a uniform layer of the glaze material on the outer and the inner diameter of the riser tube. The coated riser tube was dried in air and then fired in a resistance furnace using the recommended firing schedule for glaze 1 (Table 4.4). Unlike the results obtained in the laboratory, the riser tube cracked during the firing process. The potassium and lithium compounds used as raw materials may have dissolved in water and then deposited in the pores of the tube, encouraging cristobalite formation in DFS and causing the tube to crack. Apart from the cracking of the DFS tube, the fused sections of the glaze appeared to be grainy and lumpy, suggesting that the starting powders were too coarse. Another attempt was made to coat a large section of a riser tube with glaze 1, this time using finely ground (ball-milled) starting powders and using methyl alcohol as a solvent. The section was again dipped in the slurry, dried in air, and fired in the furnace using a similar firing schedule. This time, the DFS tube did not crack. However, the glaze did not fuse uniformly, and fine cracks formed, suggesting that the CTE mismatch between the glaze and the tube caused the crazing and spalling (see Fig. 4.26)

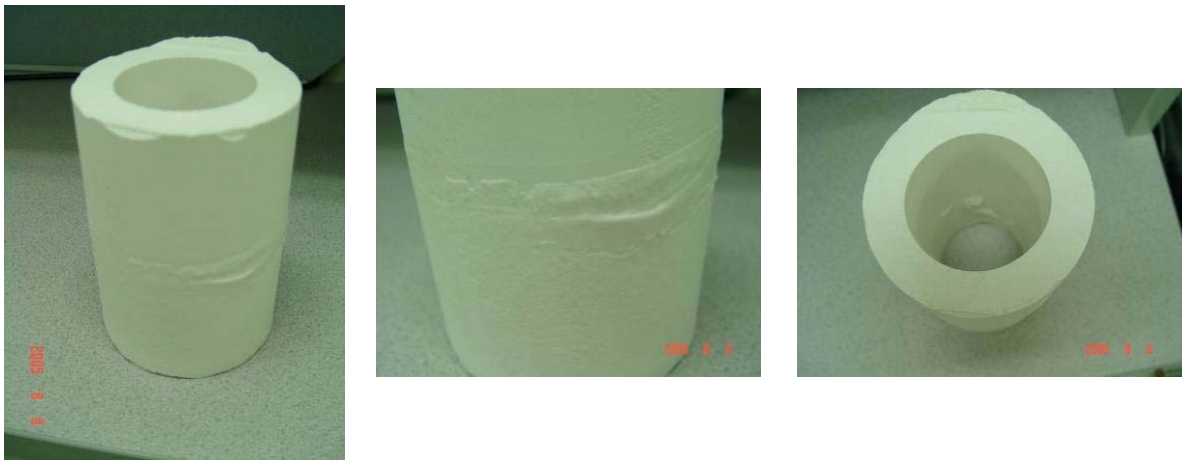

(a) (b) (c)

Fig. 4.26. A section of DFS riser tube tested with glaze 1 prepared in methanol.

While coating trials with full-scale DFS tubes using glaze 1 were unsuccessful, Pyrotek has reported positive test results with its proprietary XL glaze, a zircon-based coating material. Several DFS tubes were coated with XL glaze and tested in the field. The coatings led to life extensions of up to 300%. Pyrotek reports that an uncoated tube generally lasts for a period of 1 week, whereas XL-coated DFS tubes survive for an average period of 3 weeks. Field-testing of the coated DFS tubes consists of continuously immersing the coated tubes in molten aluminum until they start leaking. A leaking tube will produce reject castings, and the whole process must be stopped until another tube is installed to replace the leaking tube. The replacement process usually accounts for 2–4 h of lost production time. Therefore, an airtight, nonleaking tube is extremely important for reducing downtime and preventing energy losses. Pyrotek's XL-coated riser tubes have been shown to increase the life of DFS tubes, thus reducing rejection and saving energy, time, and money.

4.5.1 Advanced Monolithic Refractories

Four fused-silica castables were prepared at Pyrotek based on the formulations predicted using the optimized particle size distribution model from UMR. These castables were tested in one of the four die-casting machines at General Aluminum in Wapakoneta, Ohio. The castables ran continuously for

about 8 weeks until casting defects, such as blow holes in the sprue area, were discovered. Whether the casting defects occurred as a result of leakage in the riser tube or because of tooling stackup is not known. Pyrotek will be manufacturing four more castable tubes in the near future for additional field tests to confirm the outcome of this first test. Figure 4.27 compares the extension in the life of the riser tubes through application of coatings and the newly developed castable formulations.

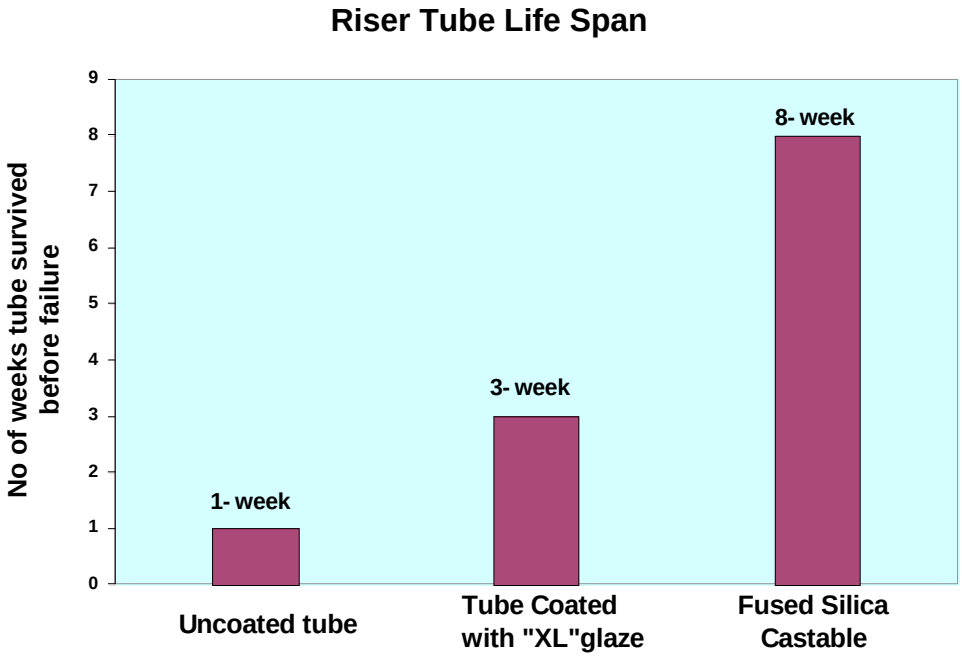

Fig. 4.27. Life extension in riser tubes resulting from coatings and castable refractories.

5. Accomplishments

5.1 Technical Accomplishments

The major technical accomplishments of the project were as follows:

- The economic feasibility of high-density infrared heating was explored. While this technique was shown to be useful in modifying the surface of the fused silica, it was not cost-effective.
- Several semicrystalline glazes were selected and applied to DFS test specimens. Preliminary results showed that the glazes are crystalline and adherent to the fused silica. One of the glazes has been identified as a potential candidate for coating application on DFS tubes. Field testing of riser tubes using this glaze, as well as the XL glaze developed at Pyrotek, has been performed.
- A permeability measuring apparatus has been developed to accommodate full-scale fused silica riser tubes and is currently being refined for use as a quality control apparatus in the riser tube production line.
- Preliminary particle size distribution analysis has been performed on several existing blends, and the information was used to develop a computer model to refine the distribution and design low-permeability castable formulations. Field-testing of castable refractory riser tubes produced using these newly designed formulations is currently under way.

5.2 Commercialization

Two cost-effective coating formulations with excellent thermal shock properties and resistance to molten aluminum attack were identified as promising candidates for application on DFS riser tubes. One coating formulation is XL glaze, a zircon-based coating materials system developed at Pyrotek; the other, referred to as “glaze 1” in this report, is a lithium silicate–based coating system that was studied at ORNL. In addition to coating formulations, a computer model suggesting optimized particle packing or particle size distribution (PSD) that would minimize permeability in monolithic fused silica castables was developed at UMR. Another outcome that evolved out of the research efforts at UMR was the development of a permeability measuring apparatus that can accommodate a full-scale DFS riser tube.

DFS riser tubes coated with the XL glaze have been commercialized and are routinely manufactured and supplied by Pyrotek to its customers. The XL-coated DFS tubes are reported to last 3–5 weeks, as compared with uncoated DFS tubes, which last only 7 days; thus, the XL glaze extends the life of the DFS tubes up to 300–400%. Additionally, four full-scale fused silica castables that were formulated on the basis of the PSD computer model were designed and manufactured at Pyrotek and are now undergoing field-testing at General Aluminum, Wapakoneta, Ohio. Preliminary test results have shown that the silica castables lasted for 8 weeks during the aluminum casting operations, indicating an increase in the lifetime of the riser tubes by 700%.

5.3 Publications

An article and a poster presentation resulted from this research. These are reproduced in Appendixes A and B.

6. Conclusions

The primary goal of this project was to develop and validate new classes of cost-effective low-permeability ceramic and refractory components for handling molten aluminum in both melting and casting environments. Three approaches were employed with partial to full success to achieve this goal:

1. Develop materials and methods for sealing surface porosity in thermal-shock-resistant ceramic refractories
2. Develop new ceramic coatings for extreme service in molten aluminum operations, with particular emphasis on coatings based on highly stable oxide phases
3. Develop new monolithic refractories designed for lower-permeability applications using controlled porosity gradients and particle size distributions

The results of the research work and the field tests performed utilizing these three approaches are listed below:

- It was demonstrated that high-density IR heating could be a tool for altering and sealing the surface porosity of fused silica. However, the process was not very cost-effective.
- A low-cost glaze composition having a coefficient of thermal expansion (CTE) similar to that of a DFS tube was identified and was successfully tested for its integrity and adherence to DFS. Although the glaze acted as a barrier between the molten aluminum and the DFS, persistent porosity and crazing within the glaze affected its performance during the reactivity tests, thus acting as an obstacle in scaling up production of this glaze.
- Pyrotek's XL glaze showed great success in improving the life of the DFS tubes. Pyrotek has reported an increasing market demand for the XL-coated DFS tubes, which exhibit useful lifetimes three times better than those of uncoated tubes.
- A computer model to optimize particle size distribution for reduced permeability was developed and successfully applied to casting formulations. Silica riser tubes produced using these new formulations have been tested in a commercial aluminum casting facility and have been reported to increase the life of the DFS tubes by 700%.
- If all the DFS riser tubes used in LPD casting of aluminum automotive components are replaced with the better, longer-lasting castable riser tubes, the potential national energy savings is estimated to be 206 billion Btu/year.

7. Recommendations

Although this project was successful in developing two new glazing materials and optimized castable formulations vital for increasing the life of the riser tubes in low-pressure foundries, the outcome of this project will be effective only if such glazing technologies and formulations are used for broader and more valuable applications. In order to achieve dramatic energy and environmental benefits, it is recommended that similar coatings or glazes and castable formulations be extended to other refractory components within the aluminum casting industry (such as troughs, metal handling ladles, spouts, and pins) as well to other industries, including glass, chemical, petrochemical, steel, agriculture, mining, and forest products. Furthermore, in terms of improving the performance of glaze 1, an additional nonwetting coating (such as BN) is suggested. For the XL glaze, additional characterization of its composition and understanding of its aluminum reactivity kinetics is recommended.

8. References

[1] R. Brindle, ed., *Applications for Advanced Ceramics in Aluminum Production: Needs and Opportunities*, report prepared for the U.S. Advanced Ceramics Association, The Aluminum Association, and DOE/OIT, February 2001.

[2] W. D. Kingery et al., *Introduction to Ceramics*, J. Wiley, Hoboken, N.J., 1976, pp. 540–48.

[3] J. G. Hemrick et al., *Refractories for Industrial Processing: Opportunities for Improved Energy Efficiency*, report prepared for DOE-EERE Industrial Technologies Program, January 2005.

[4] U.S. Department of Energy, Energy Information Agency, *1998 Manufacturing Energy Consumption Survey (MECS)*, 1998, Table No 3.2, Fuel Consumption.

[5] S. W. Hadley, S. Das, and J. W. Miller, *Aluminum R&D for Automotive Uses and the Department of Energy's Role*, ORNL/TM-1999/157, Oak Ridge National Laboratory, Oak Ridge, Tenn., March 2000.

[6] U. S. Department of Energy, Office of Industrial Technologies, *1997 Energy and Environmental Profile of the US Aluminum Industry*, Table 1.6, pp. 12, 13.

[7] R. J. Lauf and J. H. DeVan, "Evaluation of Ceramic Insulators for Lithium Electrochemical Reduction Cells," *Journal of the Electrochemical Society* 139, no. 8 (1992): 2087–91.

[8] E. M. Levin, H. F. McMurdie, and F. P. Hall, Phase Diagrams for Ceramists, American Ceramic Society, Columbus, Ohio, 1964, vol. 1, p. 122.

[9] R. J. Lauf et al., Method of Making a Functionally Graded Material, U.S. Patent Application, 2001.

[10] O-J. Siljan et al., "Refractories for Molten Aluminum Contact, Part I: Thermodynamics and Kinetics," *Refractories Applications and News* 7, no. 6 (2002): 17–25.

[11] C. A. Blue et. al., *JOM-e* 52, no. 1 (2000).

[12] E. F. O'Conor and R. A. Eppler, "Semicrystalline Glazes for Low Expansion Whiteware Bodies," *Ceramic Bulletin* 52, no. 2 (1973).

[13] R. A. Eppler and D. R. Eppler, *Glaze and Glass Coatings*, A&C Black, London, and American Ceramic Society, Westerville, Ohio, 1998.

[14] S. M. Salman and S. N. Salama, "Thermal Expansion Data of Some Alkali Aluminosilicate Glasses and Their Respective Glass-Ceramics," *Thermochimica Acta* 90 (1985): 261–76.

[15] A.W. A. El-Shennawi et al., "Crystallization of Some Aluminosilicate Glasses," *Ceramics International* 27 (2001): 725–30.

[16] J. Canon and T. Sander, "New Test Method for Evaluating Permeability of Refractory Castables," *Refract. Appl.* 2, no. 1 (1997): 6–7.

[17] J. Funk and D. Dinger, *Predictive Process Control of Crowded Particulate Suspensions Applied to Ceramic Manufacturing*, Kluwer Academic Publishers, Boston, 1994.

Appendix A:
Interaction of Aluminum with Silica-Based Ceramics

The following article appeared in Advances in Refractories of the Metallurgical Industries IV, *Proceedings of the 4th International Symposium on Advances in Refractories for the Metallurgical Industries, Hamilton, Ontario, August 22–25, 2004, pp. 221–234.*

Interaction of aluminum with silica-based ceramics

José M. Soto, Jeffrey D. Smith, William G. Fahrenholtz.
Department of Ceramic Engineering
University of Missouri-Rolla
Rolla, MO 65409-0330
USA

ABSTRACT

Interactions between A356 aluminum (Al-Si alloy) and dense fused silica (FS) riser tubes used for low-pressure casting of aluminum alloys were evaluated using a sessile drop approach. The tubes have a short service life, but cost and thermal shock resistance make them an effective solution. The main problem encountered during use is the reaction of aluminum with silica to form alumina and silicon, which causes failure. Tests have been conducted on as-fired (uncoated) and modified (coated) tubes. Experiments were carried out in a horizontal furnace at 1225ºC under argon to minimize the effect of the aluminum oxide on the interactions at the alloy-silica interface. Images of the drop were acquired and contact angle values were estimated for uncoated and coated samples, but no significant differences in the contact angles were observed. Scanning electron microscopy revealed the presence of cracks at the interface between the reaction zone and the unreacted silica. The presence of reaction products (silicon in the reacting alloy and aluminum in a reaction zone between the alloy and the unaffected silica) has been confirmed using energy-dispersive spectroscopy. A two layer coating system was found to be effective in reducing penetration of the aluminum alloy.

INTRODUCTION

In the year 2000, the production of aluminum in the US was of about 10.3 million tonnes, or roughly 43% of the worldwide production of 24 million tonnes [1]. Like many other materials, production of aluminum metal, parts and components is an energy-intensive process and it generates waste, including spent refractory ceramics. Over the last decade research was conducted with the aim of increasing the efficiency and reducing the generation of waste in the production of aluminum [1-2]. Environments in the production of aluminum are highly corrosive and the high temperature of operations make ceramic materials, which are resistant to both the temperature and chemical aggressiveness, the contact material of choice for many parts of the aluminum production process. It has been recognized that there is a need for a better understanding of the aluminum/ceramic interactions [3]. Ceramics are used in aluminum smelting and holding operations as well as in the downstream processes.

One of these downstream processes is casting. More specifically, refractory materials for the low-pressure casting of aluminum alloys are investigated in the present research. The casting device consists of an airtight sealed chamber where a crucible containing the molten metal is placed. A casting device is attached to the top of the chamber. A tube (riser) in the bottom of the casting device extends down into the liquid metal in the crucible. A positive pressure of ~15 psi is applied inside the chamber, which makes the molten metal flow through the riser up into the mold. Defects such as porosity in the as-fired tube or cracks generated by the reaction of the Al alloy with the tube material lead to tube failure because the pressure drop needed to force the aluminum alloy up into the casting apparatus cannot be supported due to the increased permeability of the tubes. A schematic of the process is shown in Figure 1.

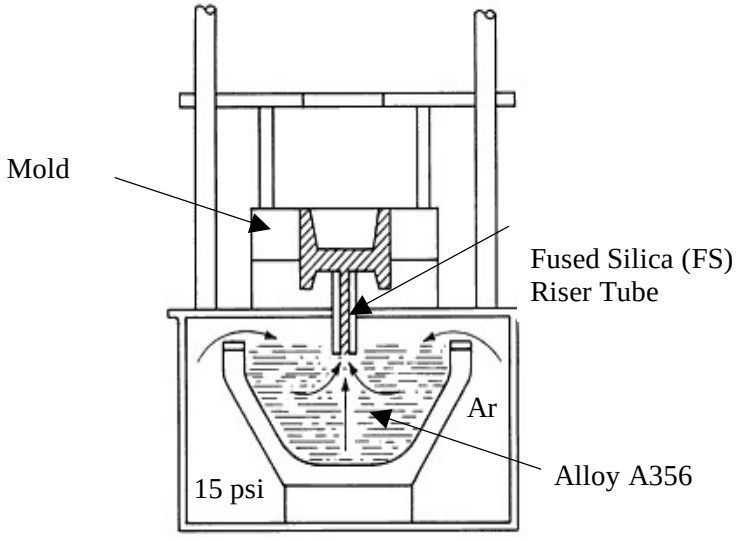

Figure 1 – Schematic of a low-pressure casting apparatus for aluminum alloys [4]

Risers have been made of a variety of ceramics and even metals. Alloy A356 is a common aluminum-silicon alloy used in low-pressure casting. Currently, dense fused silica tubes prepared by slip casting are widely used as risers.

Although slip cast fused silica tubes have a short service life their cost makes them an effective solution. The main problem associated with silica is the formation of alumina and silicon in a penetrated zone. The reaction results in cracking at the reaction interface due to the difference in specific volume between the reaction zone (mainly Al_2O_3) and the bulk of the ceramic (SiO_2). The reaction also produces contamination of the metal as it has been reported by other researchers [5-10]. According to Siljan et al. [9] aluminum reacts with silica to form alumina and silicon according to the reaction:

$$4Al_{(l)} + 3SiO_2 = 2Al_2O_3 + 3Si \quad \Delta G_{1200K} = -503.1 \text{ kJ/mole} \qquad (1)$$

Aluminum and its alloys are in the liquid state below temperatures of 700ºC. Although aluminum is readily oxidized at atmospheric conditions, industrial processes involve turbulence and fluid flow that continuously break the oxide layer allowing the liquid metal to contact the surface of the ceramic.

In the static conditions of laboratory tests like the sessile drop test, the formation of a layer of oxide on the surface of the molten metal will prevent contact between molten metal and the surface of the ceramic. In previous studies [11-12] one way this problem was overcome has been to increase the temperature and reduce the partial pressure of oxygen to promote the formation of the gaseous oxide Al_2O instead of solid Al_2O_3. Prabriputaloong and Piggott [12] indicated that at 1073 K and a partial pressure of oxygen around 10^{-5} mbar Reaction 2 will proceed:

$$4Al_{(l)} + SiO_2 = 2Al_2O_{(g)} + Si \qquad \Delta G_{1073K} = -414 \text{ kJ/mole} \qquad (2)$$

Prabriputaloong and Piggott [12] also indicated that at 1073 K and under low oxygen partial pressure the preexisting Al_2O_3 layer could decompose according to the reaction:

$$Al_2O_3 + 4Al_{(l)} = 3Al_2O_{(g)} \qquad \Delta G_{1073K} = -88 \text{ kJ/mole} \qquad (3)$$

In the present research, a sessile drop test was used as a preliminary tool to evaluate the interaction between aluminum alloy A356 and fused silica riser tubes. Contact angle values were estimated from pictures taken at 1225ºC and scanning electron microscopy and energy-dispersive spectroscopy was used to evaluate the microstructure and composition of the reaction zone.

EXPERIMENTAL PROCEDURE

Samples were received as rings taken from fused silica riser tubes. Rings were 7.5 cm internal diameter and 2.3 cm wall thickness. Three different kinds of samples were received: as-fired, tubes with a single-layer coating and tubes with a two layer coating. Specimens in the shape of ring sections of approximately 1.4 cm width in the inner diameter were cut from all the rings (See Figure 2).

Figure 2 - Specimens cut from rings of riser tubes

The nominal composition of alloy A356 is shown in Table I. Cubes of the aluminum alloy A356 of about 1 gram in weight were cut from a billet as shown in Figure 3.

Table I - Nominal Composition of Alloy A356 [13]

Element	Si	Fe	Cu	Mn	Mg	Zn	Ti	Others		Al
								each	total	
%	6.5-7.5	0.6	0.25	0.35	0.20-0.45	0.35	0.25	0.05	0.15	balance

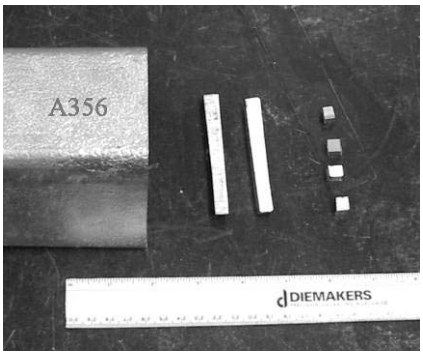

Figure 3 – Aluminum alloy cubes cut from billet

All the silica specimens were dried at 140 ºC for at least 24 hours before testing to remove adsorbed water from any porosity. The fused silica section of the ring, with its inner diameter facing up, was place in a small ceramic pan bedded with granular alumina and leveled as illustrated in Figure 4.

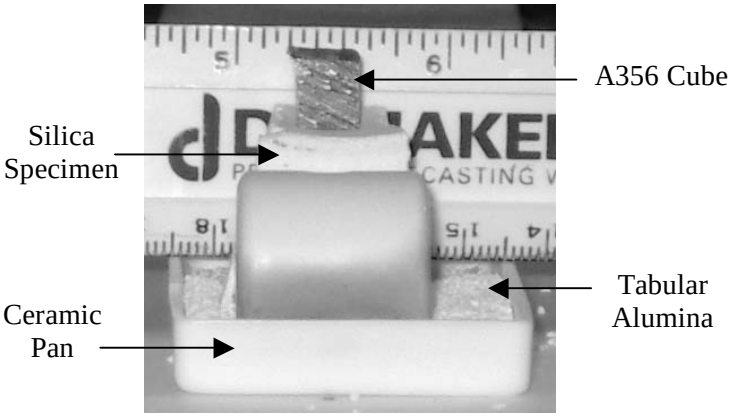

Figure 4 – Placement of alloy cubes on top of the specimens.

A sealed horizontal furnace coupled with a gas purifier was used to heat the sample to the test temperature. The experimental set up can be seen in Figure 5.

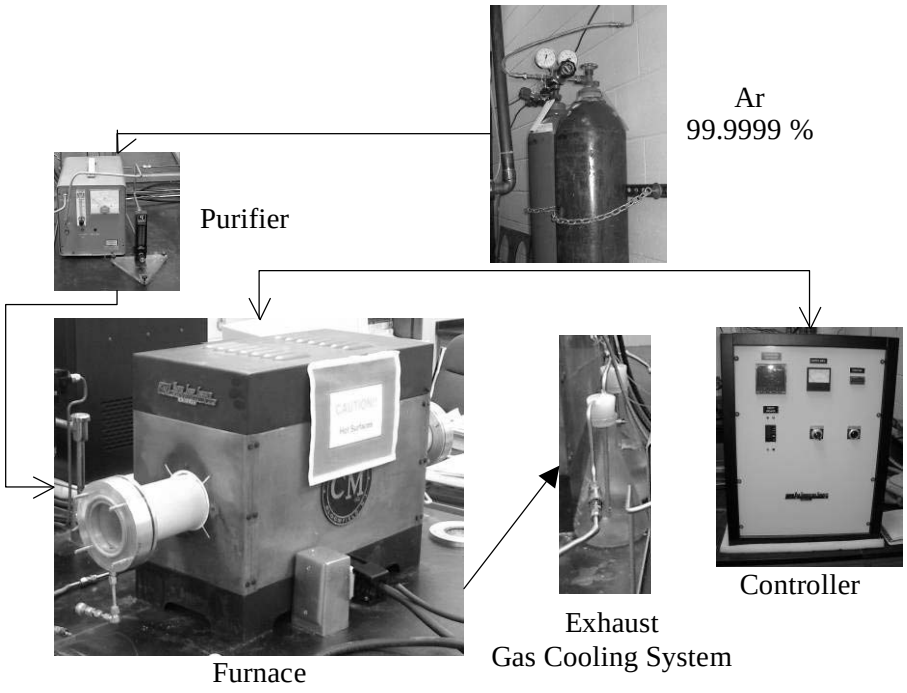

Figure 5 – Experimental set up for wetting and reaction experiments.

For the contact angle experiments, furnace temperature was programmed to increase at 5 ºC/minute until reaching 1225 ºC and then held at 1225 ºC for 60 minutes. Temperature was monitored with an optical pyrometer that read an average specimen temperature of 1138 ± 10 ºC during the contact angle experiments. The difference between the programmed temperature and the pyrometer temperature was expected since the thermocouples that control the furnace temperature are outside the ceramic tube and colder argon gas was continuously flowed through the furnace tube. The furnace tube was equipped with transparent windows at both ends. A digital video camera (Sony DCR-TRV140) was used to record the shape of the drop a regular intervals between 600ºC and 1225ºC. Images for contact angle estimations were captioned from the video taken after the samples

had been at the hold temperature for at least 30 minutes. Angles were measure using Scion Image software. Four measurements from each image were made and the average and standard deviation calculated.

After the contact angle measurements were completed, specimens were cooled to room temperature. Once they were cool, specimens were embedded in epoxy and then sectioned perpendicular to the metal-ceramic interface. Macro pictures of the cross sections were taken to determine depth of penetration. Cross section were dried, polished and coated with carbon for examination by scanning electron microscopy (SEM) and energy-dispersive spectroscopy (EDS).

RESULTS AND DISCUSSION

Typical penetration results are shown in Figure 6 for as-fired tubes as well as those with single and two layer coatings. Figure 7 shows the macro images of the different kinds of sample tested.

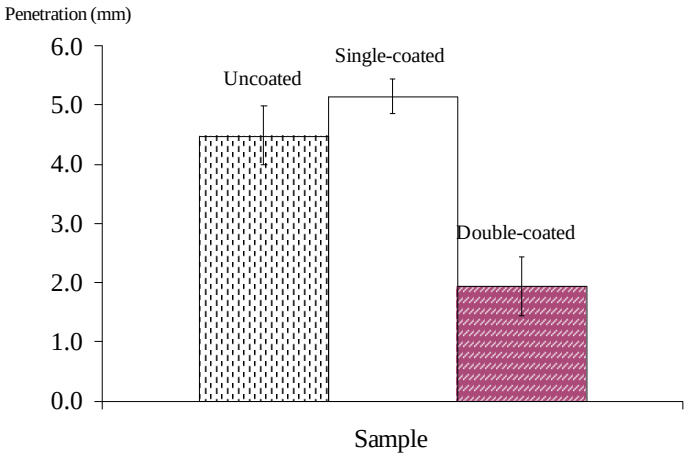

Figure 6 – Quantitative comparison of average depth of penetration (and deviation) for the as-fired, single layer, and two layer riser tubes.

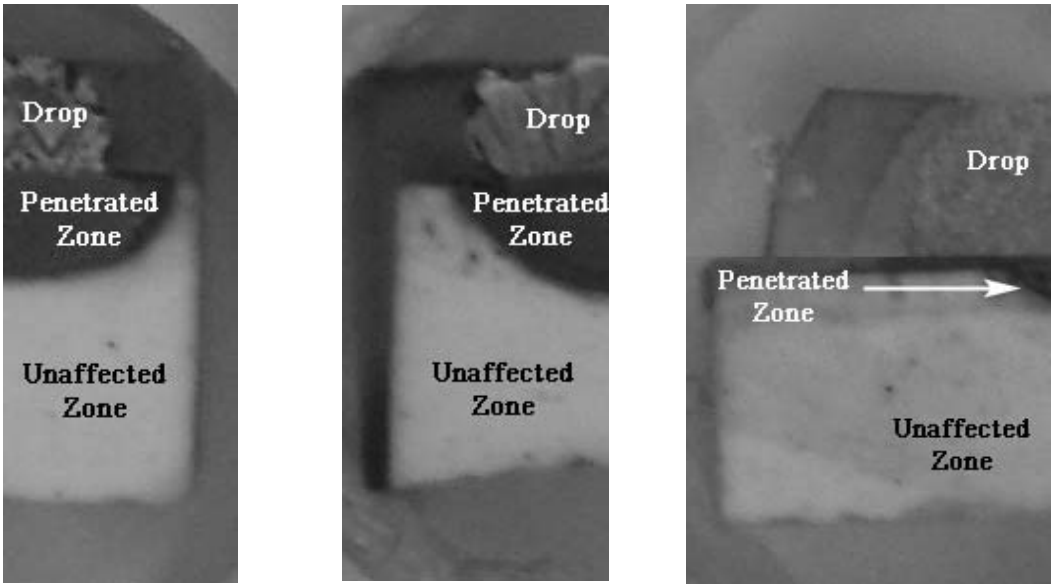

(a) As-fired uncoated (b) Single coating (c) Double coating

Figure 7 – Qualitative comparison of depth of penetration for the as-fired, single layer, and two layer riser tubes.

It can be seen that the difference in penetration between the uncoated specimen and the specimen with the single layer coating is not significant. However, the sample with the two layer coating had less penetration than the other two sample types. The two layer coating seems to effectively prevent the contact between the liquid aluminum alloy and the silica substrate.

Figure 8 show superimposed images of drops from test with the three different specimens and Table II shows the estimated values for the contact angle.

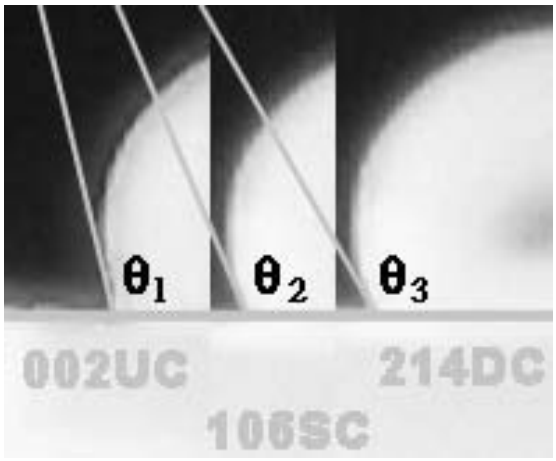

Figure 8 - Qualitative comparison of apparent contact angles.

Table II. Measured apparent contact angles.

Specimen	Contac Angle
Uncoated 002UC	$\theta_1 = 121 \pm 3$ degrees
Single Coating 106SC	$\theta_2 = 121 \pm 6$ degrees
Double Coating 214DC	$\theta_3 = 125 \pm 5$ degrees

Although the images show slight difference in contact angles for the three types of substrates, the average values do not vary significantly when considering the standard deviations of measurements from multiple specimens. The uncoated specimens and the tubes with the single layer coating have the same average contact angle. Specimens with the two layer coating have a slightly higher average contact angle, but the error bar for the three specimens overlap as it is shown in Figure 9.

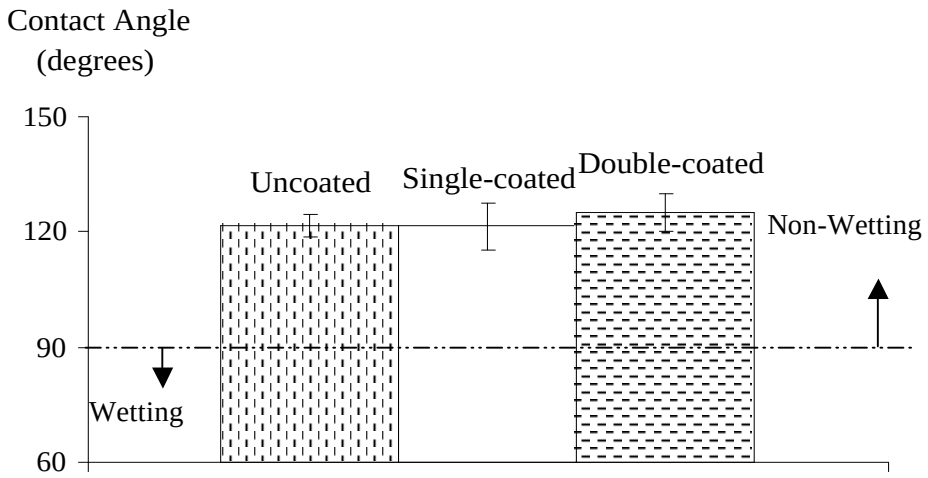

Figure 9 – Comparison of apparent contact angles.

The reaction of the molten drop with the substrate produced a groove around the drop reduced the accuracy of the contact angle measurements.

The initial microstructure of the aluminum alloy is shown in Figure 10. The dark rounded features are pores. EDS mapping showed that discrete Si-rich particles were present in the aluminum matrix.

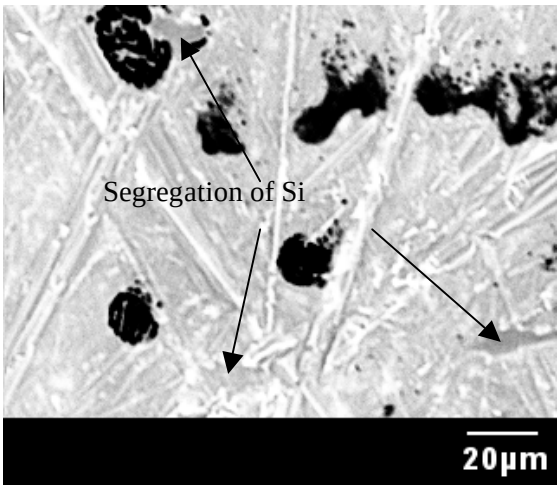

Figure 10 - Microstructure of aluminum alloy 356 before testing.

Figure 11 shows the condition of the body of the fused silica slip cast tube before testing. EDS analysis confirmed that the material was ~100% silica. Silica particles as big as ~200 µm are observed. Also pores as big as ~50 µm are present.

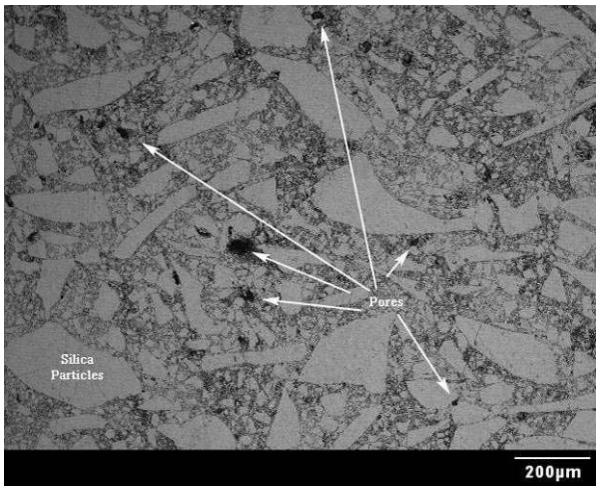

Figure 11 - Microstructure of the dense fused silica tube prior to testing

Figure 12 shows the uncoated sample after testing. Silicon crystals produced by reaction of the metal with the silica substrate have grown all the way through the original Al drop. The reaction zone (RZ) contained aluminum in the form of alumina and some residual metal. Cracks were observed at the interface between the reaction zone and the unaffected fused silica. Cracks were generated by the difference in specific volume between silica and alumina.

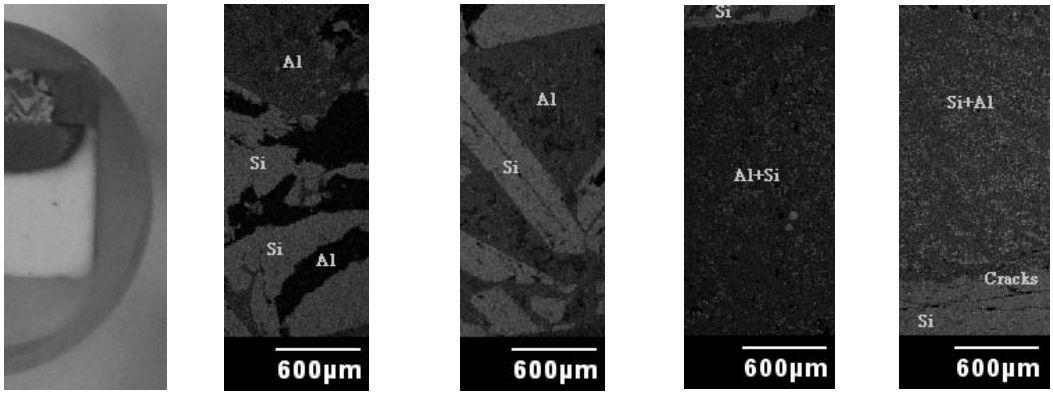

EDS Compositional Maps (Al, Si)

(a) Macro (b) Drop Top (c) Drop Bottom (d) RZ Top (d) RZ Bottom

Figure 12 – SEM micrographs for the as-fired uncoated FS tube after testing

The initial condition of the sample with the single layer coating is shown in Figure 13. Figure 13(b) is a backscattered electron image that shows the differences in composition between the coating (top, darker) and the bulk FS (bottom, lighter). The coating was around 120 µm thick and contains Zr and Ca.

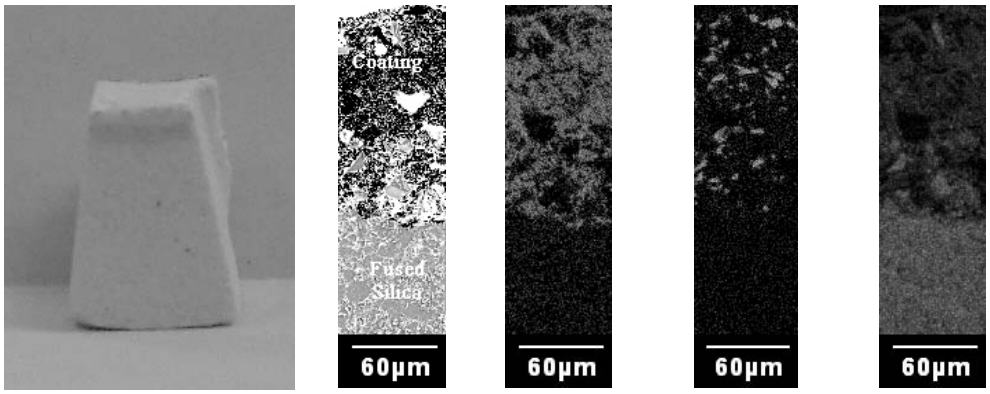

(a) Macro (b) BEI (c) Zr Map (d) Ca Map (e) Si Map

Figure 13 – Initial condition of the sample with the single layer coating

Figure 14 shows the condition of the sample with the single layer coating after testing. Relatively large (~ 200 µm width and greater than 600 µm length) silicon crystal can be seen inside the drop. As with the uncoated sample, the reaction zone contained aluminum and silicon. Cracks were present at the interface between the reaction zone and the underlying fused silica.

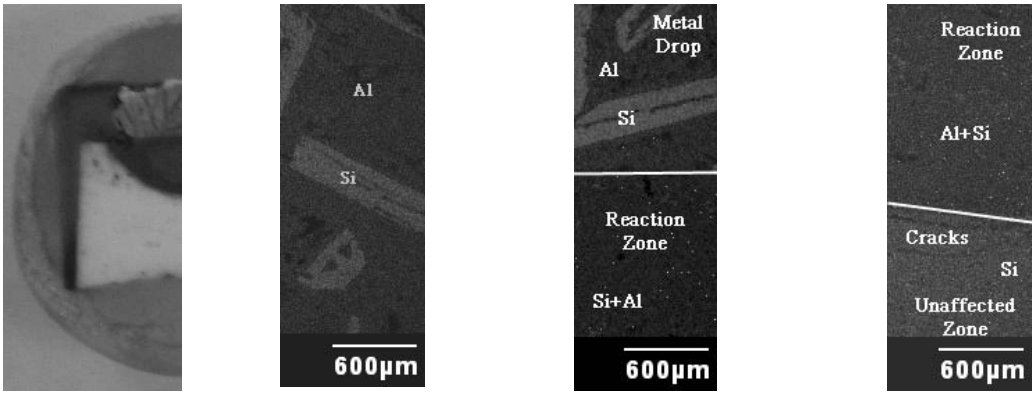

EDS Compositional Maps

(a) Macro (b) Drop (c) Interface Drop-RZ (d) Interface RZ-FS

Figure 14 – SEM micrographs and EDS compositions for the FS tube with the single layer coating after testing.

The initial condition of the sample with the two layer coating is shown in Figure 15. Figure 15(b) is a backscattered electron image that shows the differences in composition between the coating (top, darker) and the bulk of the FS (bottom, lighter). The first layer of the coating was around 10µm thick and contained Zr and Ca while second layer was around 30 µm thick. The two layers have different compositions.

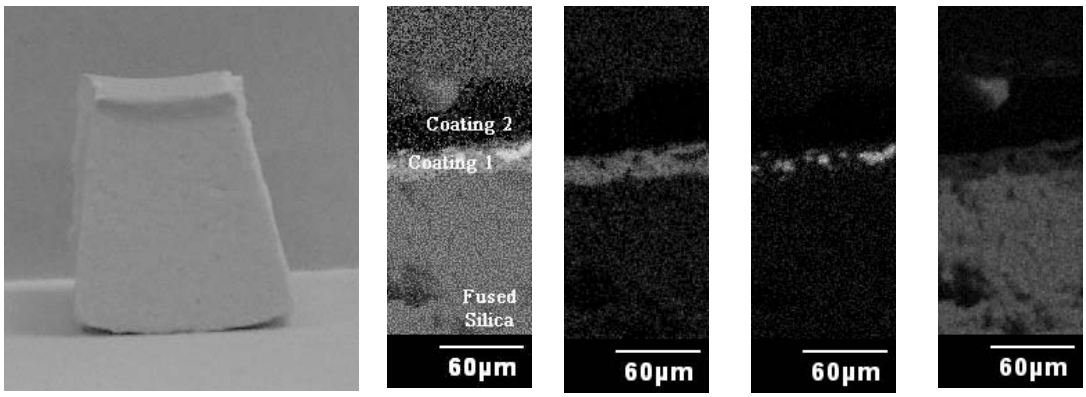

EDS Compositional Maps

(a) Macro (b) Whole (c) Zr (d) Ca (e) Si

Figure 15 – Initial condition of the sample with the single layer coating

Figure 16 shows the sample with the two layer coating after testing. Only a small silicon crystal can be seen inside the bottom of the residual Al drop. As with the other samples, the reaction zone contained aluminum and silicon. Cracks were present at the interface between the reaction zone and the unaffected fused silica.

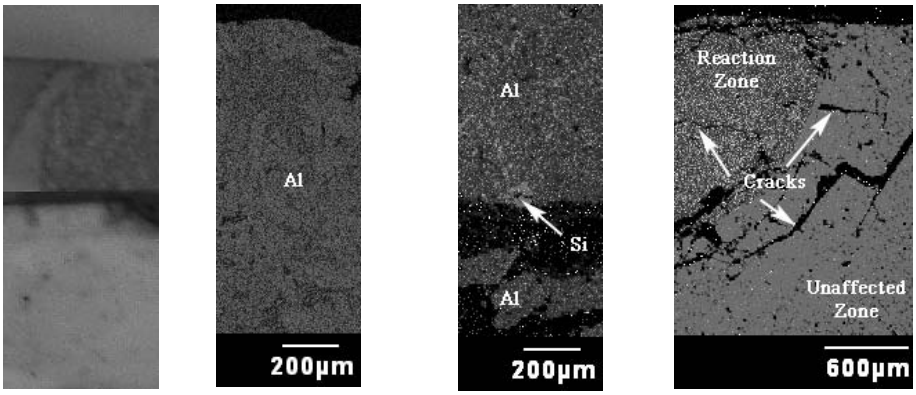

EDS Compositional Maps (Al, Si)

(a) Macro (b) Drop Top (c) Drop Bottom (d) RZ Side

Figure 16 – SEM micrographs for the FS with the two layer coating after testing.

CONCLUSIONS

Aluminum alloys react with and penetrate into FS riser tubes used in the low pressure casting of aluminum. This interaction results in the formation of a reaction zone and an increased Si content in the alloy. Samples with a two layer coating experienced less penetration than samples either with a single layer coating or without any coating. No changes were observed in contact angle for the three types of specimens.

This research is ongoing. Other coatings and alternative materials will be evaluated. Also, the effects of initial tube permeability, the presence of open or closed porosity will be evaluated along with a comparison of thermal shock resistance and tensile strength among all of the materials tested.

AKNOWLEDGEMENTS/DISCLAIMER

This material is based upon work supported by the U.S. Department of Energy and Pyrotek, Inc. under award number DE-PS07-01ID14244. Any opinions, findings, and conclusions or recommendations expressed in this material are those of the authors and do not necessarily reflect the views of the Department of Energy.

REFERENCES

1. Aluminum Vision Steering Committee of the Aluminum Association, Aluminum Industry Vision, Sustainable Solutions for a Dynamic World, November 2001.
2. The Aluminum Association, Aluminum Industry Technology Roadmap, February 2003.

3. United States Advanced Ceramics Association, The Aluminum Association and U.S. Department of Energy, Applications for Advance Ceramics in Aluminum Production: Needs and Opportunities, February 2001.
4. ASM International, Materials Handbook Desk Edition, 2001, pages 748-749.
5. Brondyke, K.J., "Effect of Molten Aluminum on Alumina-Silica Refractories". Journal of the American Ceramic Society, Vol. 36, No. 5, 1953, 171-175.
6. Fouletier, M.; Gold, D., "Selective, Accelerated Test for Evaluation of Refractory Lifetime in Contact with Aluminum Alloys" UNITECR'91, Proceedings of the Unified International Conference on Refractories, Aachen, Germany, 1991, 36-38.
7. Pereira, A.P.F.A.; Baldo, J.B., UNITECR'97, Proceedings of the Unified International Conference on Refractories, New Orleans, USA, 1997, 1667-1676.
8. Angers, R.; Tremblay, R.; Desrosiers, L.; Dube, D., "Interactions between Dense Alumina-Silica Ceramics and Molten Aluminum", Journal of the Canadian Ceramic Society, Vol. 66, No. 1, February 1997, 64-71.
9. Siljan, O-J.; Rian, G.; Petersen, D.T.; Solheim, A.; Schoning, C., "Refractories for Molten Aluminum Contact Part I: Thermodynamics and Kinetics", Refractories Applications and News, Volume 7, No. 6, November/December 2002, 17-25.
10. Quesnel, S.; Allaire, C.; Afshar, S., "Criteria for Choosing Refractories in Aluminum Holding and Melting Furnaces", Light Metals 1998, Addendum Section of the Proceedings of the TMS, 391-1402.
11. Coudurier, L.; Adorian, J.; Pique, D.; Eustathopoulos, N., "Etude de la Mouillabilite par L'aluminum Liquide de L'alumine et de L'alumine Recouverte d'une Couche de Metal ou de Compose Refractaire", Revue Internationale des Haute Temperatures, Vol. 21, No. 2, 1984, 81-93.
12. Prabriputaloong, K.; Piggott, M.R., "Thin-film Studies of the Reduction of SiO2 by Al", Journal of the American Ceramic Society, Vol. 56, No. 4, 1973, 177-180.
13. ASTM International, ASTM B 108 – 03a Standard Specification for Aluminum-Alloy Permanent Mold Castings, Annual Book of ASTM Standards, Volume 02.02, 2003.

Appendix B:
Development of Cost-Effective Low-Permeability Ceramic and Refractory Components for Aluminum Melting and Casting

The following poster presentation appeared at ITP 2004, Materials, Glass, Sensors Project and Portfolio Review Meeting, Arlington, Virginia, June 21–24, 2004.

Development of Cost-Effective Low-Permeability Ceramic and Refractory Components for Aluminum Melting and Casting

D. Brown[1], G. Hodren[1], R. Ott [2], P. Kadolkar [2], V. K. Sikka[2], J. Smith[3] and B. Fahrenholtz[3]
[1]Pyrotek, Inc. Trenton, TN
[2]Oak Ridge National Laboratory, Oak Ridge, TN
[3]University of Missouri-Rolla, Rolla, MO

Goals and Objective

The focus of this project is to develop and validate new classes of cost-effective low-permeability ceramic and refractory components for handling molten aluminum in both smelting and casting environments. The primary goal is to develop materials and methods for sealing surface porosity in thermal shock-resistant ceramic refractories, which will also include the evaluation of monolithics used in the low-pressure casting of aluminum.

Benefits

Enhancement of the pressure-holding capacity of fused silica tubes and their implementation in aluminum melting and casting will accomplish the following:

- Reduced downtime through longer life and reduction in scrap through lower rates of erosion and particulate generation
- Reduction in the overall energy use by improving casting operations (energy savings of 30 trillion Btu/year by 2020)
- Produce results that will also enhance the performance of refractories in the aluminum, glass, and chemical industries.

Applications

Improved ceramic and refractory components from this program will be applicable to many industries.

Aluminum and Metal Casting

- Melting and casting of aluminum and its alloys.

Chemical and Petrochemical

- Improved corrosion resistance to enhance performance of several types of chemical reactors.

Glass

- Potential for enabling oxy-fuel firing.

Funding

Overall Cost

Year	DOE	Cost Share	Total
1	$233,750	$233,750	$467,500
2	$278,750	$278,750	$512,500

Cost Breakdown of DOE Funding

Year	ORNL	Subcontract to University
1	$128,667	$105,083
2	$167,704	$109,046

RESEARCH SPONSORED BY THE U.S. DEPARTMENT OF ENERGY, ASSISTANT SECRETARY FOR ENERGY EFFICIENCY AND RENEWABLE ENERGY, OFFICE OF INDUSTRIAL TECHNOLOGIES, INDUSTRIAL MATERIALS FOR THE FUTURE PROGRAM UNDER CONTRACT DE-AC05-00OR22725 WITH UT-BATTELLE, LLC.

Research Tasks

High-Density Infrared (HDI) Plasma Arc Lamp Processing

104,000 Joules – Side view

40,000 Joules – Top view

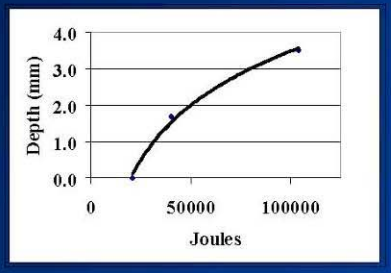

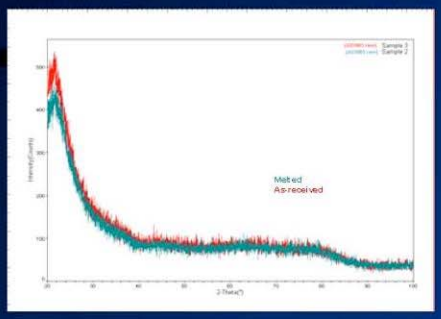

Samples were treated with HDI (high density infrared) plasma under varying processing conditions

HDI Plasma melted the surface of the specimens forming a dense layer of SiO_2

X-RD of the as-received and HDI treated samples showed that the surface heat-treatment maintains the amorphous structure of fused silica

The depth of the melt zone (see graph above) can be tailored depending on the process parameters such as lamp amperage and exposure time – correlating to energies

Semi-crystalline Glazes

A glaze material with low coefficient of thermal expansion (CTE) <0.5 /°C was selected

- CTE depends on the crystalline phases and the content of glassy matrix within the glaze
- Al_2O_3 (29.2 wt.%), B_2O_3 (5 wt.%), K_2O (5 wt.%), Li_2O (11.3 wt.%), SiO_2 (49.5 wt.%)

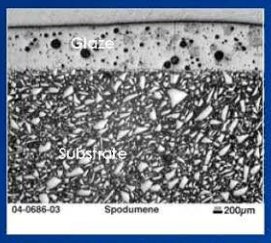

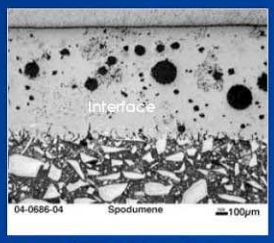

Micrographs showing the glazed surface of fused silica. Melting of glaze prior to reaching the decomposition temperature prevents escape of gases, such as CO_2, resulting into porosity

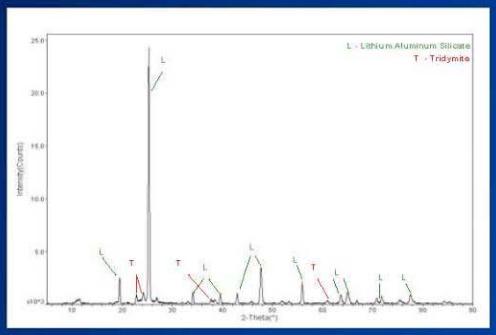

X-RD pattern shows presence of lithium aluminum silicate which has a very low $\Delta G_{reaction}$ with Al

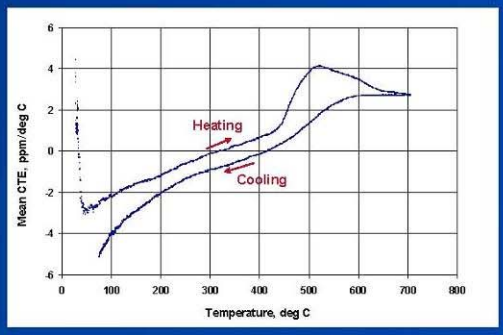

Thermal expansion measurement of monolithic glazes show negative values at low temperatures

Aluminum Reactivity Studies

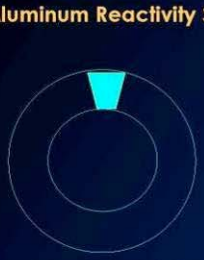

Samples were left in molten Al at 750 °C for 24, 48 and 72 hrs

A wedge-shaped piece was cut out from an inch thick cross-section of the fused silica stalk tube

One surface of the wedge-shaped piece was glazed and tested for wetting and reactivity with molten Al

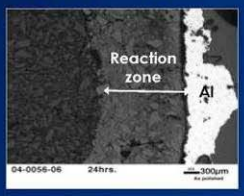

Molten Al reacting with unglazed surface of fused silica

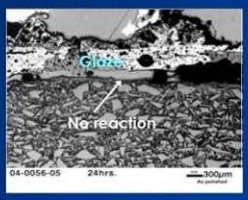

Glaze prevents attack from molten Al up to 24 hrs. Porosity and fine cracks within the glaze provide a pathway for metal penetration

Permeability Measurement

Full scale permeameter capable of measuring permeability of the full scale tube

$$K = \frac{\eta \ln(R_o / R_i) Q}{2 \pi L \Delta P}$$

η = fluid viscosity
R_o = tube outer radius
R_i = tube inner radius
Q = volume flow rate
L = tube length
ΔP = differential pressure across tube wall

Q is determined from dP/dt and the system volume

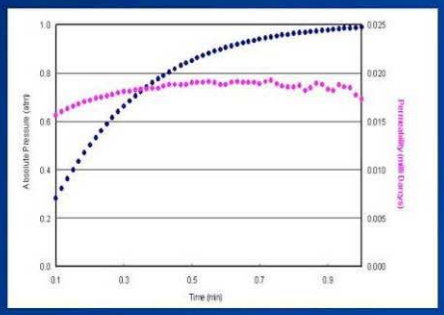

Formula developed to measure permeability
–Assumptions
- System obeys Darcy's Law
- Constant thickness cylinder

Particle Size Distribution

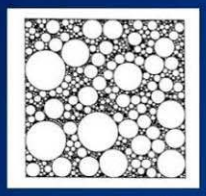

Computer model for selection of optimum aggregate to minimize permeability

Castable Formulations

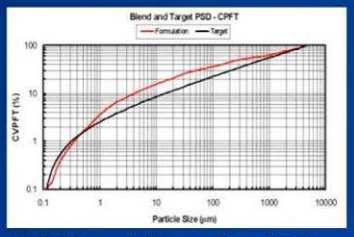

Initial Formulation vs. Target PSD

Deviation within each size class

Future Plans

- Pre-reacting or fritting of the glaze will be carried out to decompose the glaze mixture prior to its application. Fritting might prevent pore formation and produce a uniform defect-free glaze
- Other materials with low coefficient of thermal expansion such as Spodumene mineral and aluminum titanate will be tested for coatings

imf INDUSTRIAL MATERIALS FOR THE FUTURE

Pyrotek

ornl Oak Ridge National Laboratory

U. S. DEPARTMENT OF ENERGY